Electronic Supplementary Material (ESI) for Inorganic Chemistry Frontiers.
This journal is © the Partner Organisations 2024

Supplementary material

New Cyclometalated Ru(II) Polypyridyl Photosensitizers Trigger Oncosis in Cancer Cells by Inducing Damage of Cellular Membranes

Jakub Cervinka[a,b], Alba Hernández-García,[c] Delia Bautista,[d] Lenka Markova[b], Hana Kosthunova[b], Jaroslav Malina [b], Jana Kasparkova[b,e], M. Dolores Santana,[c] Viktor Brabec,[b,e] Jose Ruiz[c]

[a]*Faculty of Science, Department of Biochemistry, Masaryk University, CZ-62500 Brno, Czech Republic;*
[b]*Czech Academy of Sciences, Institute of Biophysics, CZ-61265 Brno, Czech Republic;*
[c]*Departamento de Química Inorgánica, Universidad de Murcia, and Murcia BioHealth Research Institute (IMIB-Arrixaca), E-30100 Murcia, Spain;*
[d]*ACTI., Universidad de Murcia, E-30100, Murcia, Spain.*
[e]*Department of Biophysics, Faculty of Science, Palacky University, Slechtitelu 27, CZ-78371 Olomouc, Czech Republic*

Table of contents

Synthetic procedures

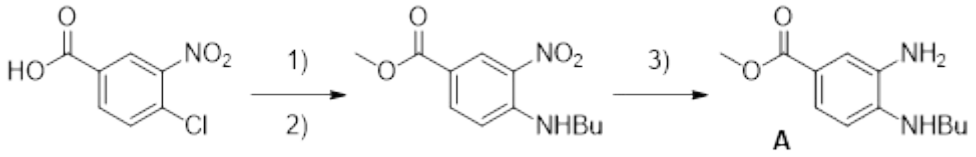

Scheme S1. Synthetic procedure for A. Reaction conditions: 1) H_2SO_4 (cat), MeOH, 65 ºC, overnight; 2) $BuNH_2$, Et_3N, CH_2Cl_2, 72 h, N_2 atm., r.t.; 3) Zn (powder) $HCOONH_4$, AcOEt/MeOH N_2 atm., 24 h, 50 ºC.

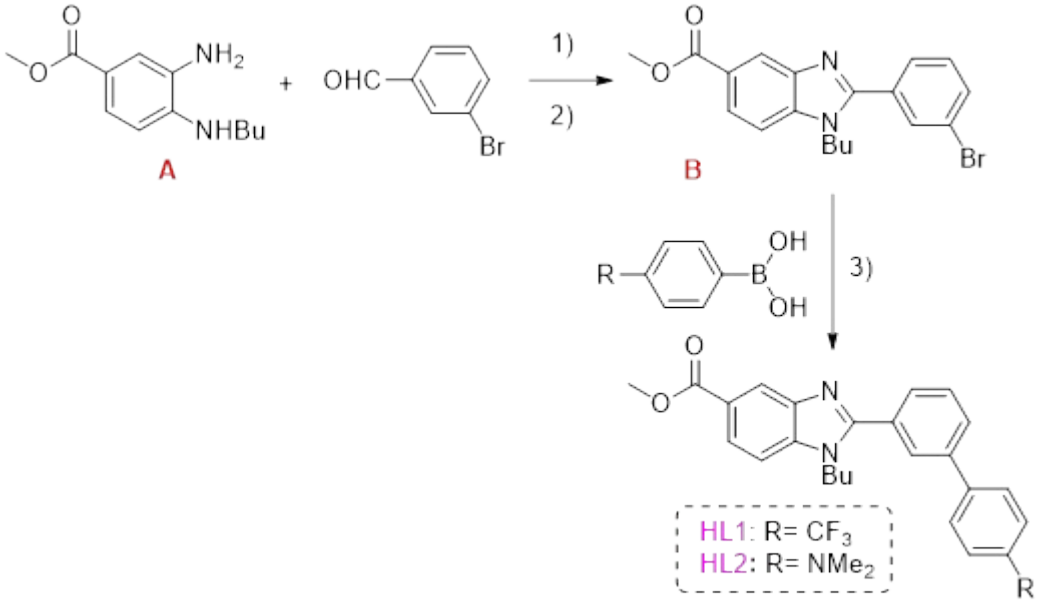

Scheme S2. Synthetic procedure for **HL1** and **HL2.** Reaction conditions: **1**) $NaHSO_3$, H_2O, 90 ºC, 1 h; **2**) EtOH: H_2O 1:1, 90 ºC overnight; **3**) $Pd(PPh_3)_4$, K_2CO_3, Toluene:H_2O 4:2, MW, 180 ºC, 1 h.[1,2]

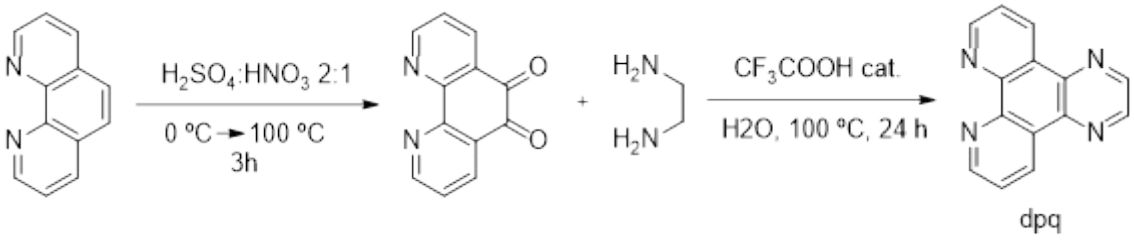

Scheme S2. Synthesis procedure of **dpq**.[3]

Characterization of ligands and complexes

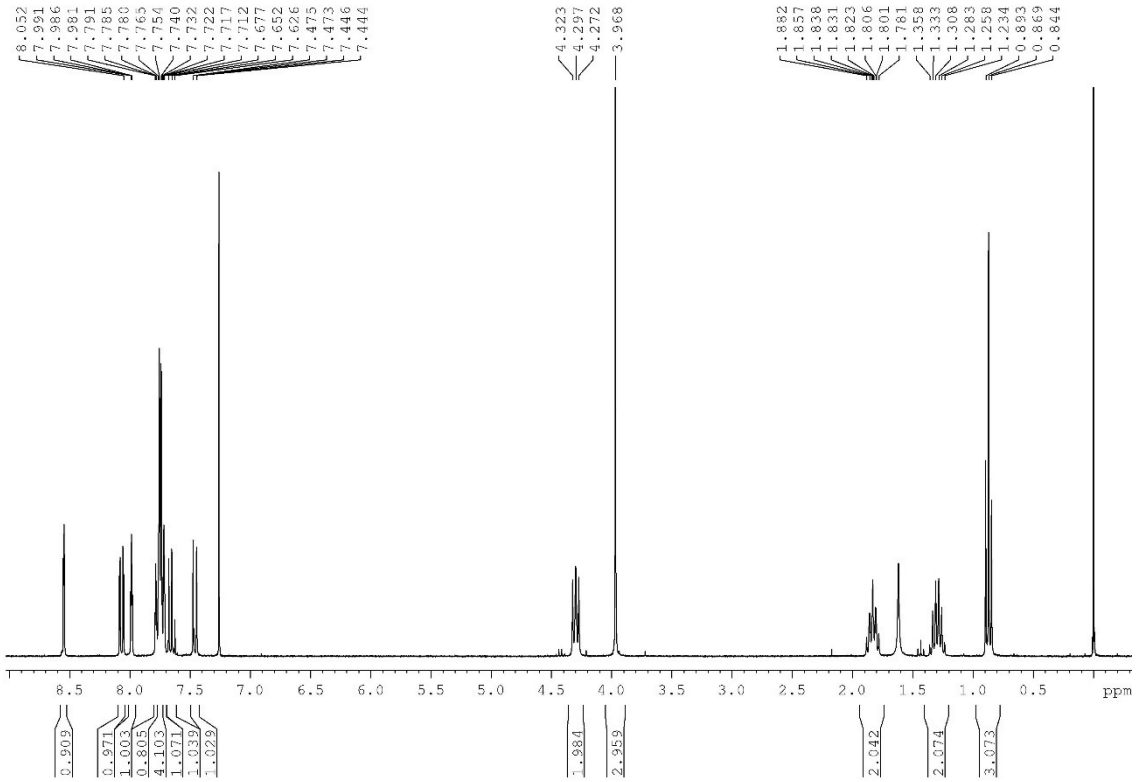

Figure S1. ^{1}H NMR of **HL1** in $CDCl_3$

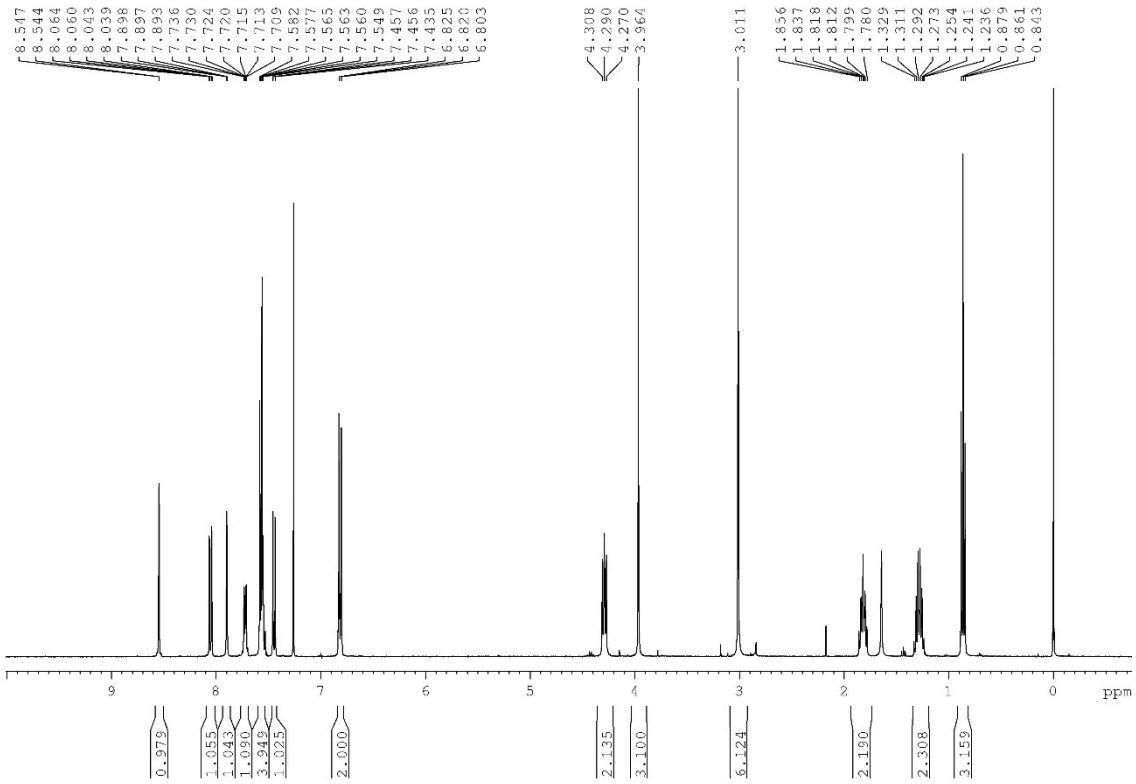

Figure S2. ^{1}H NMR of **HL2** in $CDCl_3$

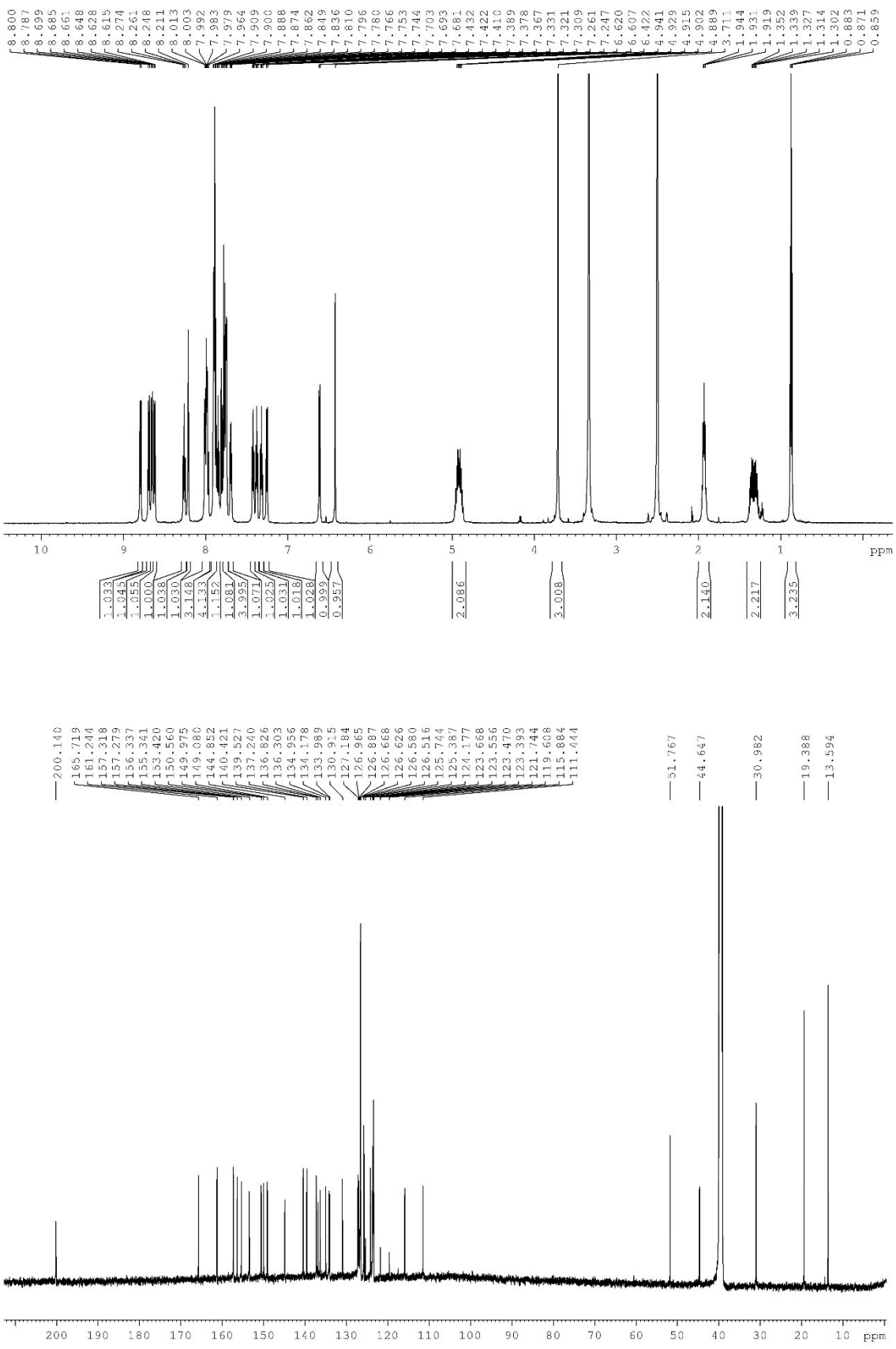

Figure S3. ^{1}H (top) and ^{13}C NMR (bottom) spectra of compound **Ru1** in DMSO-d_6

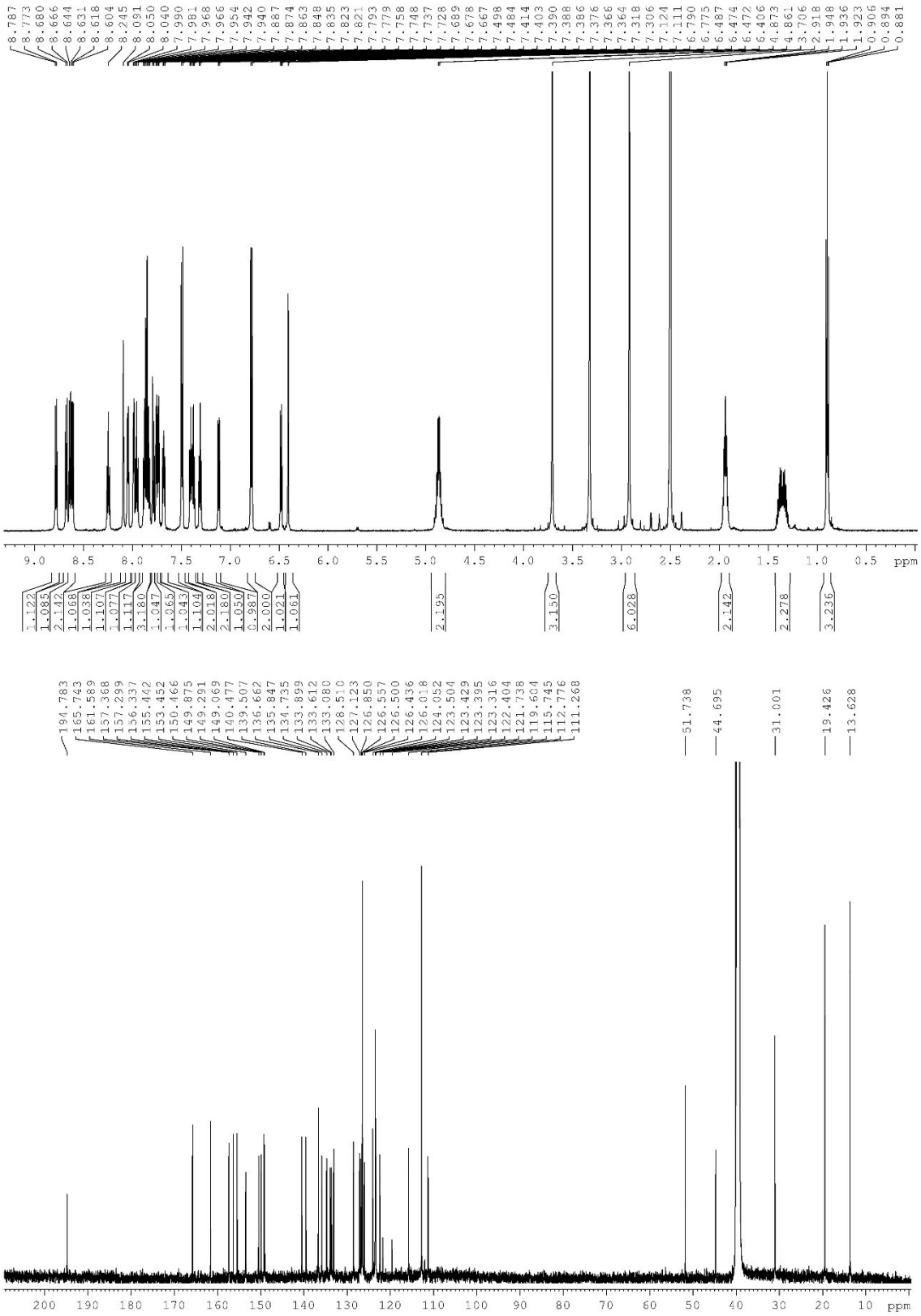

Figure S4. ^{1}H (top) and ^{13}C NMR (bottom) spectra of compound **Ru2** in DMSO-d_6.

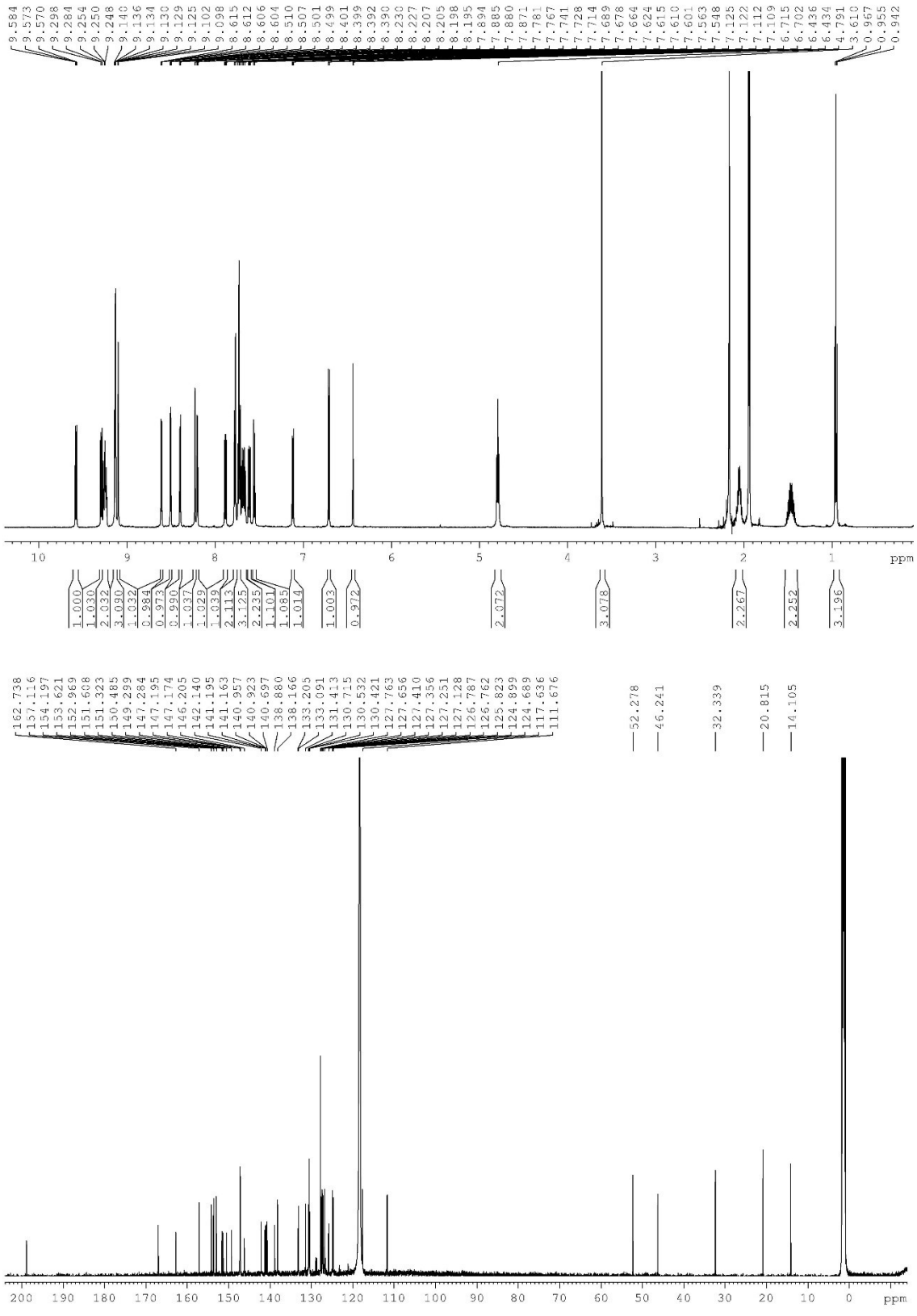

Figure S5. ^{1}H (top) and ^{13}C-NMR (bottom) spectra of compound **Ru3** in CD_3CN

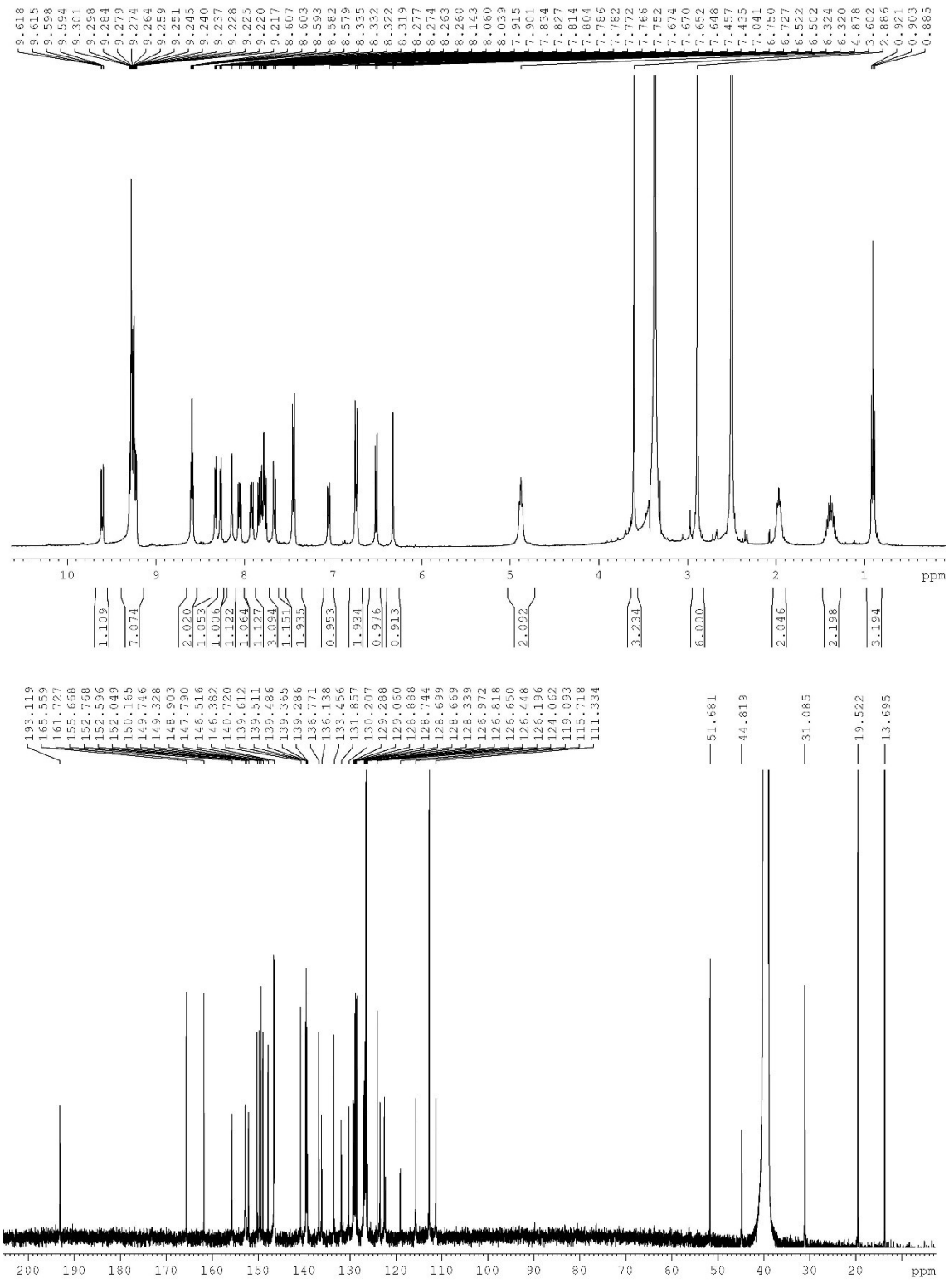

Figure S6. ^{1}H (top) and ^{13}C NMR (bottom) spectra of compound **Ru4** in DMSO-d_6

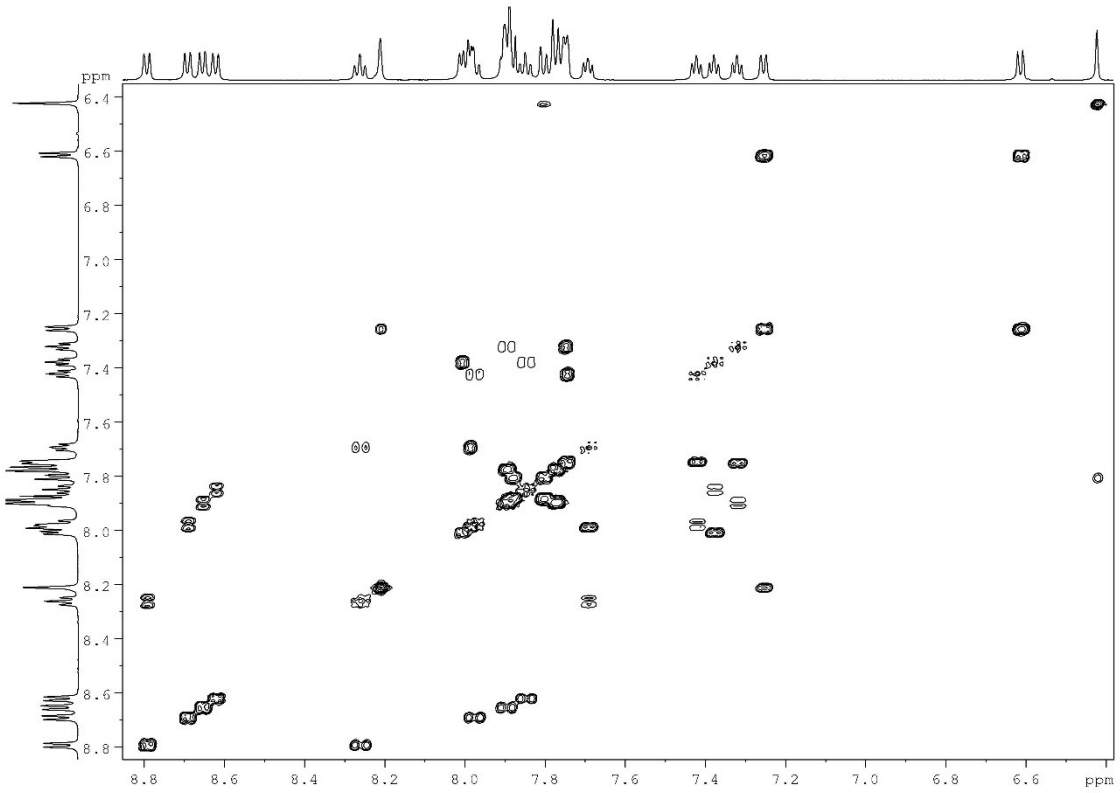

Figure S7. {^{1}H-^{1}H}-COSY NMR spectrum of compound **Ru1** in DMSO-d_6

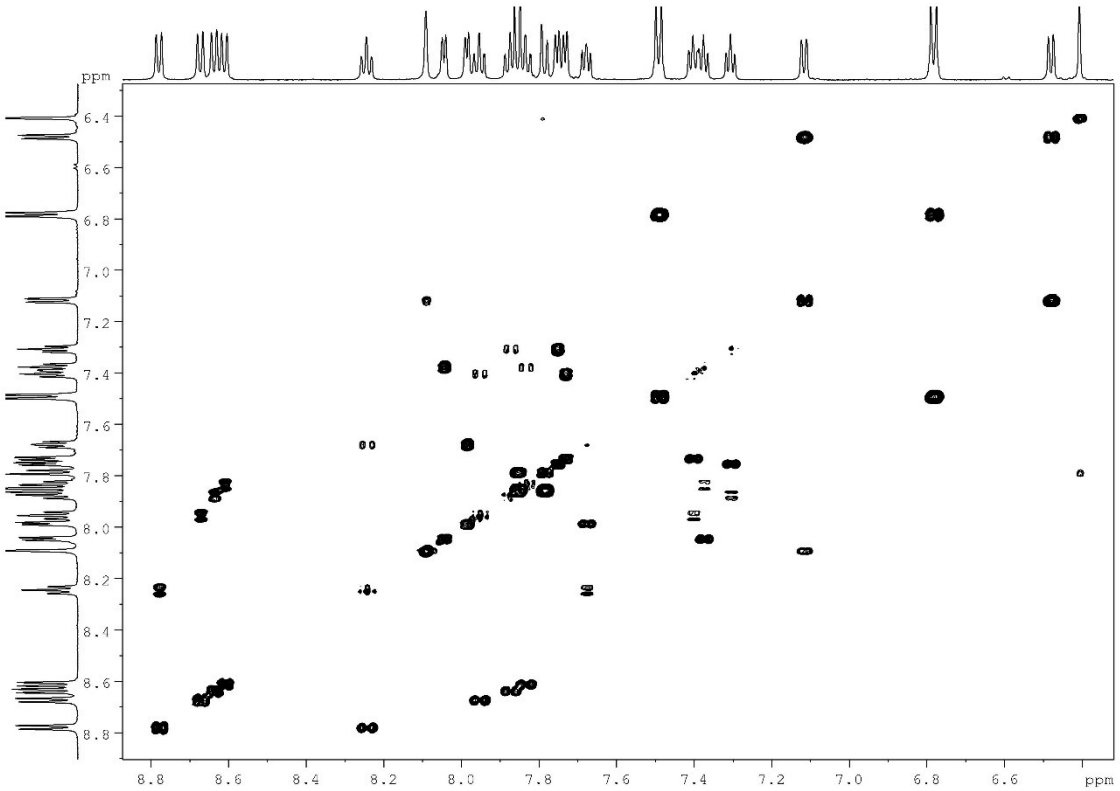

Figure S8. {^{1}H-^{1}H}-COSY NMR spectrum of compound **Ru2** in DMSO-d_6

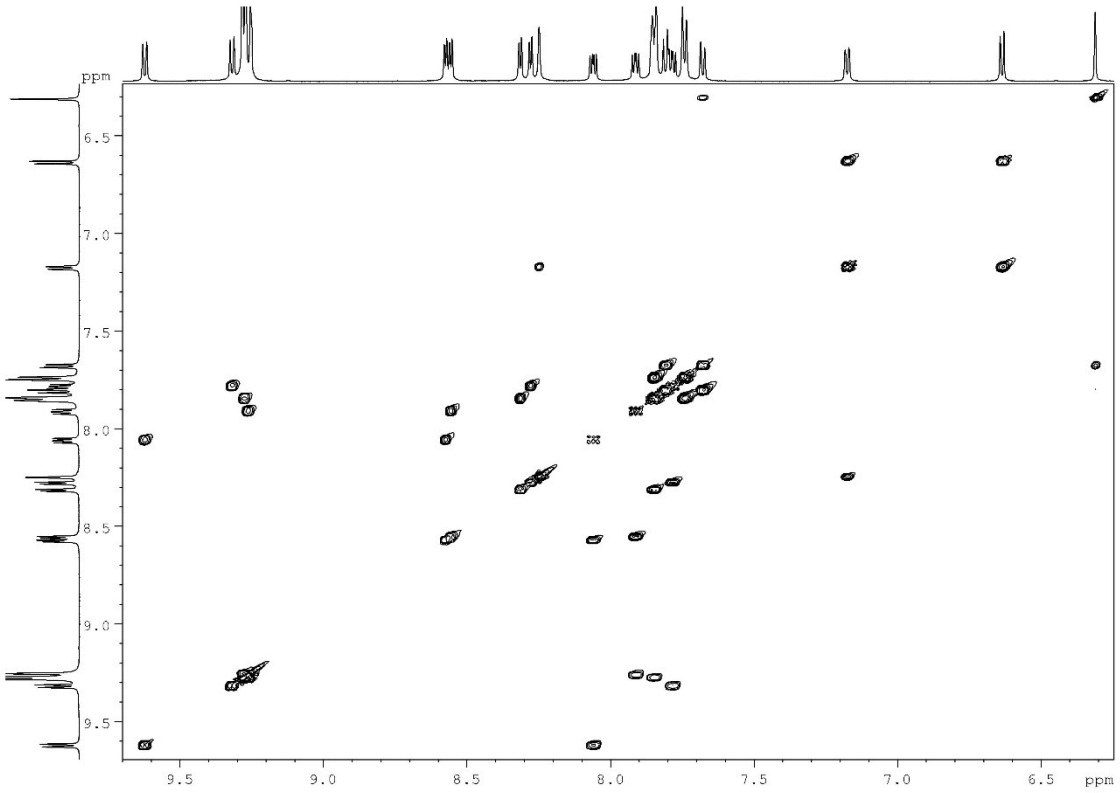

Figure S9. {^{1}H-^{1}H}-COSY NMR spectrum of compound **Ru3** in DMSO-d_6

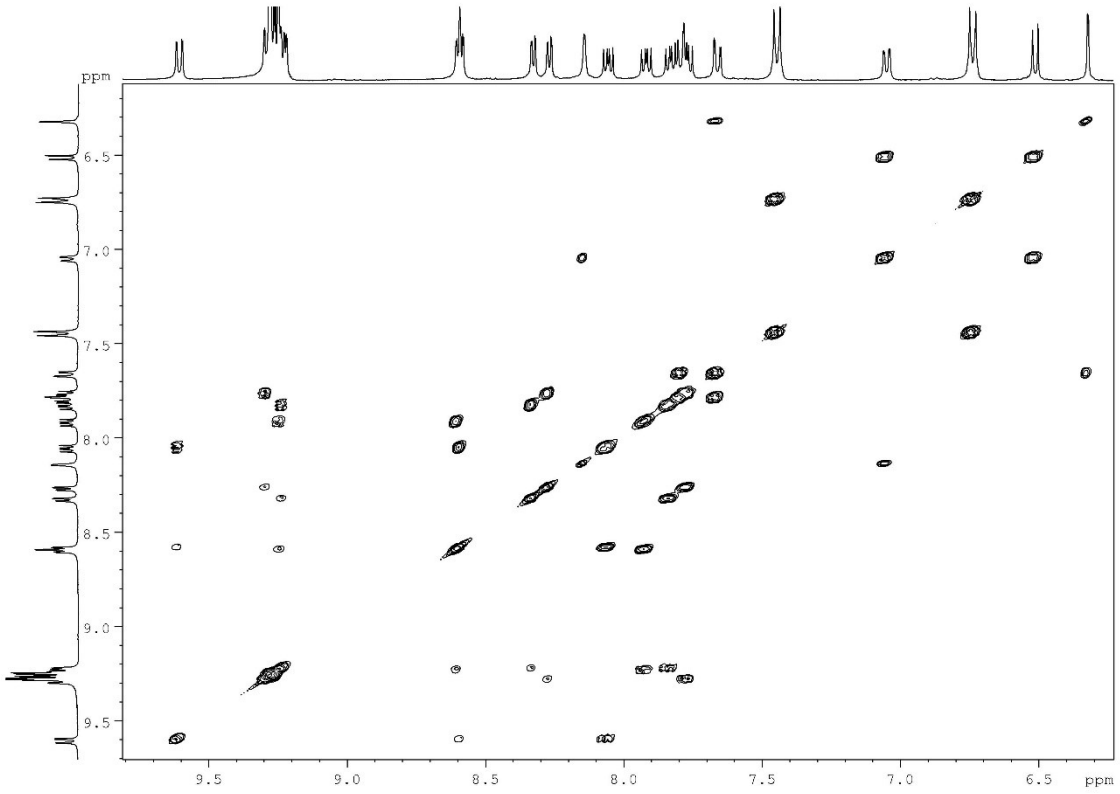

Figure S10. {^{1}H-^{1}H}-COSY NMR spectrum of compound **Ru4** in DMSO-d_6

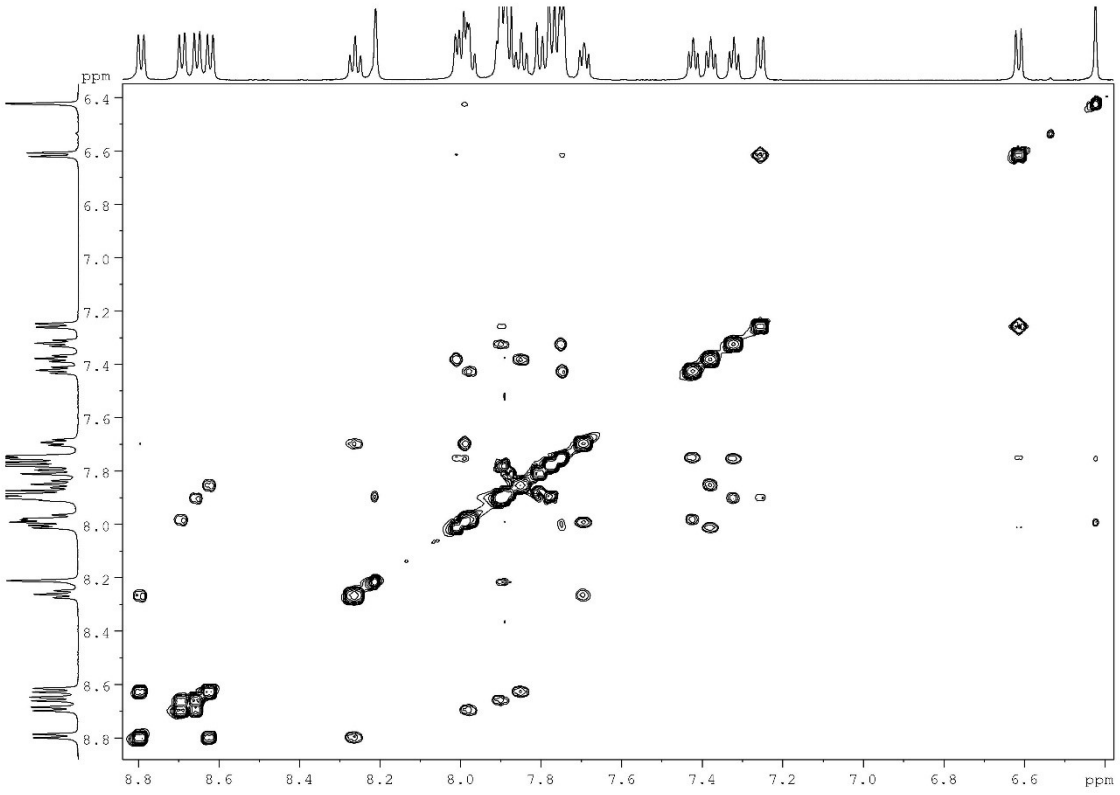

Figure S11. {^{1}H-^{1}H}-NOESY NMR spectrum of compound **Ru1** in DMSO-d_6

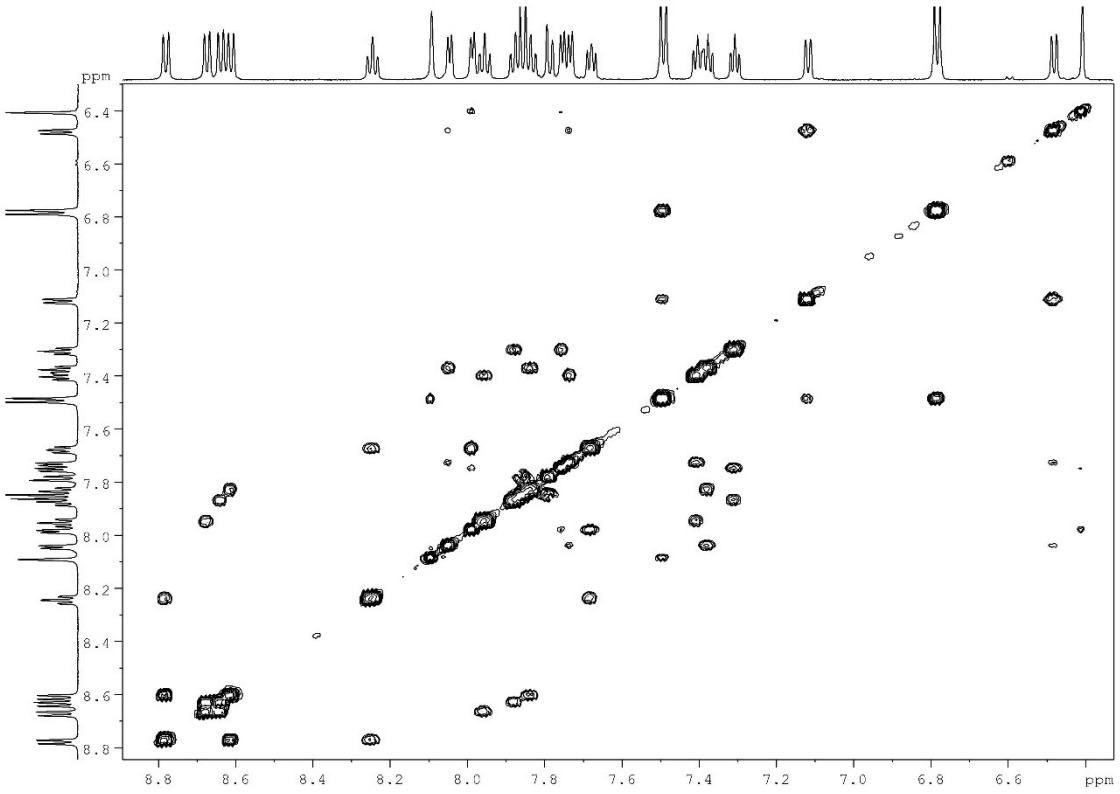

Figure S12. {^{1}H-^{1}H}-NOESY NMR spectrum of compound **Ru2** in DMSO-d_6

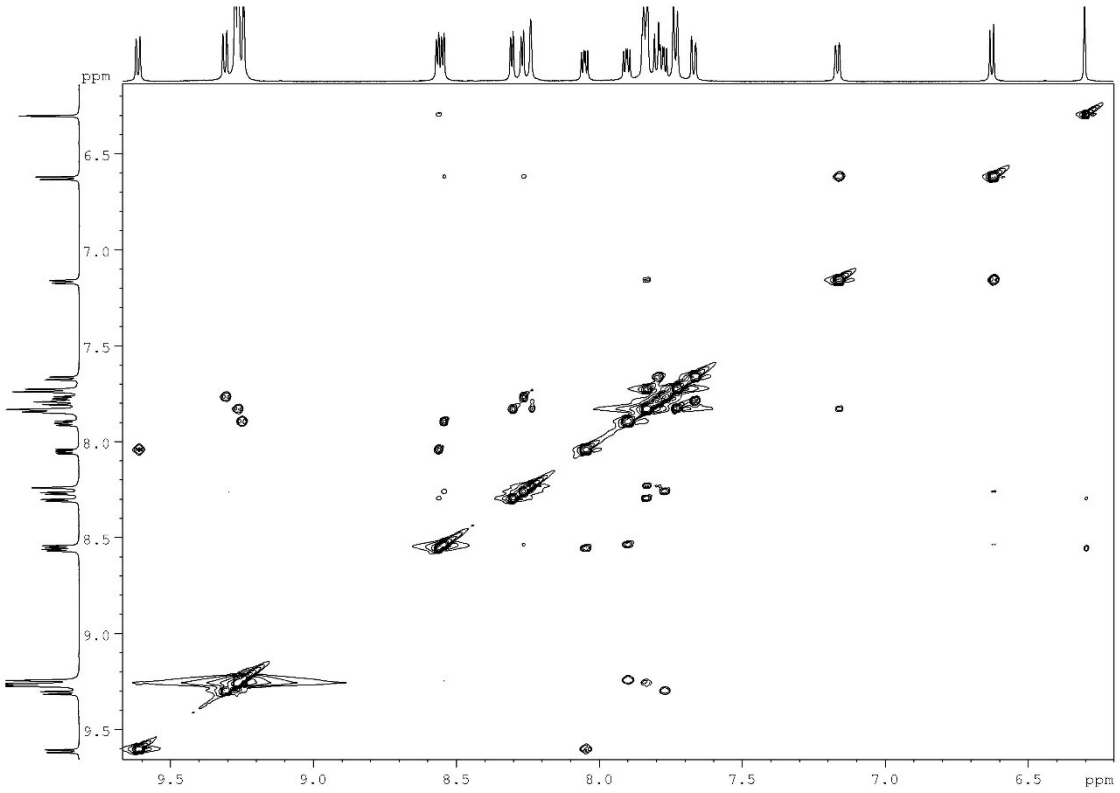

Figure S13. {^{1}H-^{1}H}-NOESY NMR spectrum of compound **Ru3** in DMSO-d_6

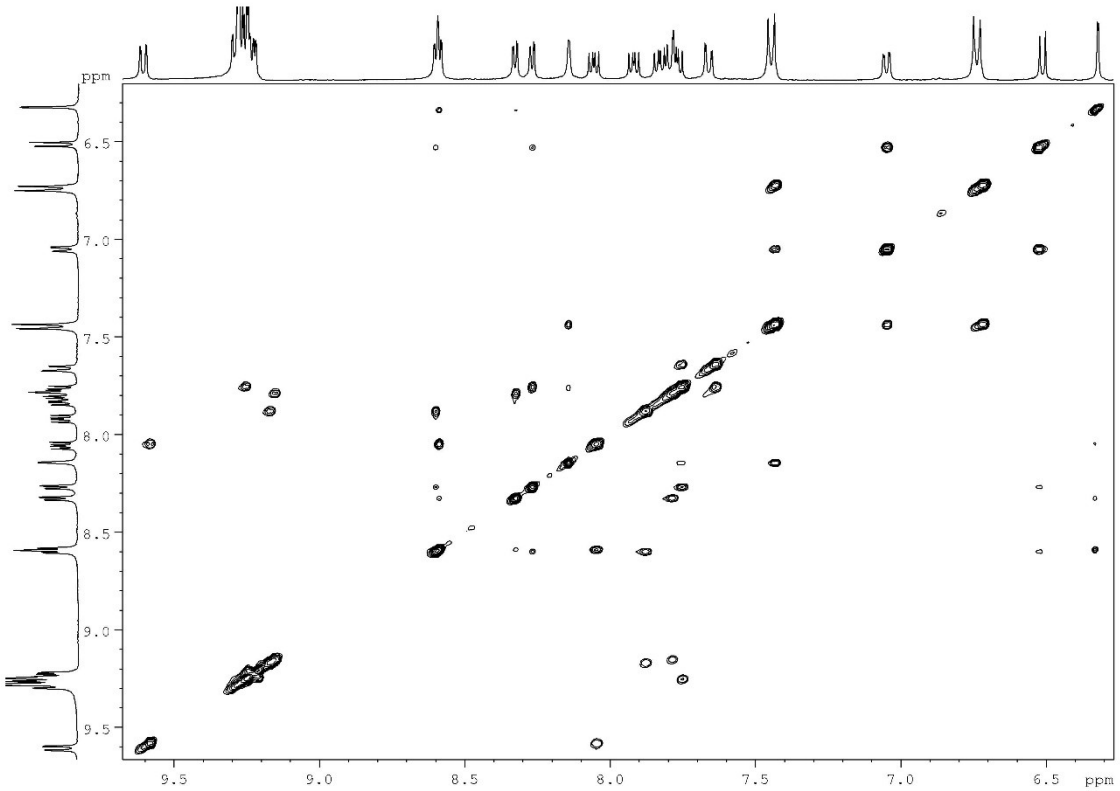

Figure S14. {^{1}H-^{1}H}-NOESY NMR spectrum of compound **Ru4** in DMSO-d_6

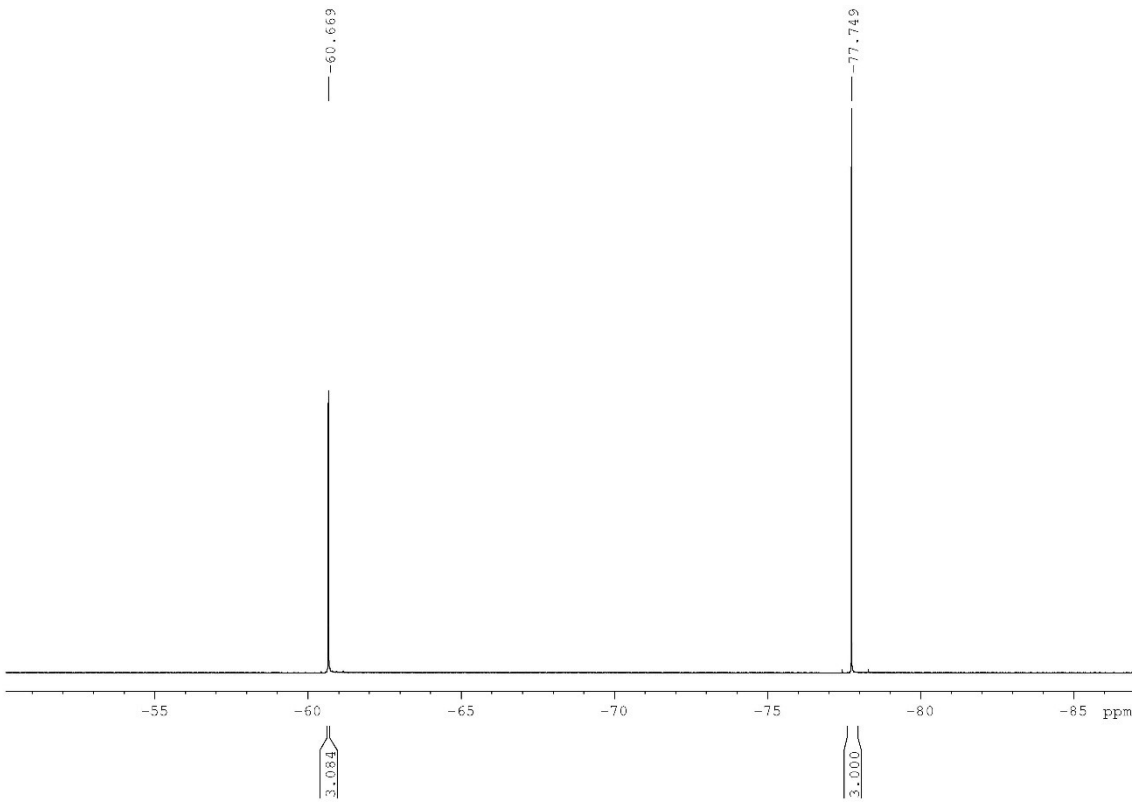

Figure S15. ^{19}F NMR spectrum of compound **Ru1** in DMSO-d_6

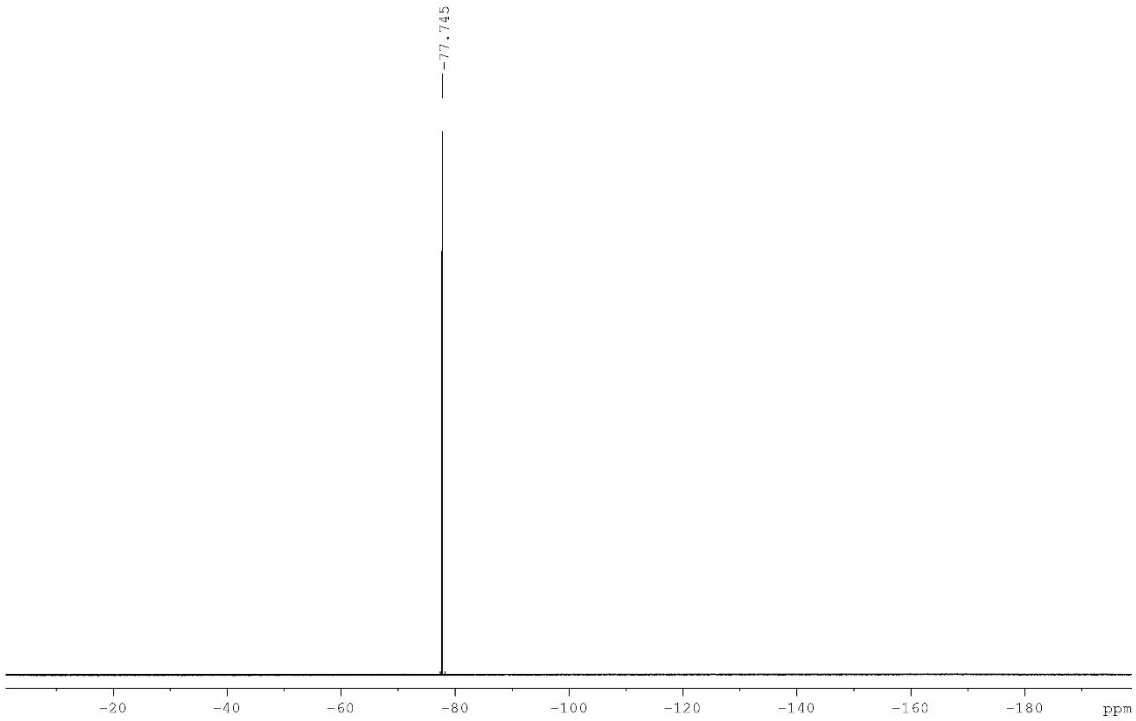

Figure S16. ^{19}F NMR spectrum of compound **Ru2** in DMSO-d_6

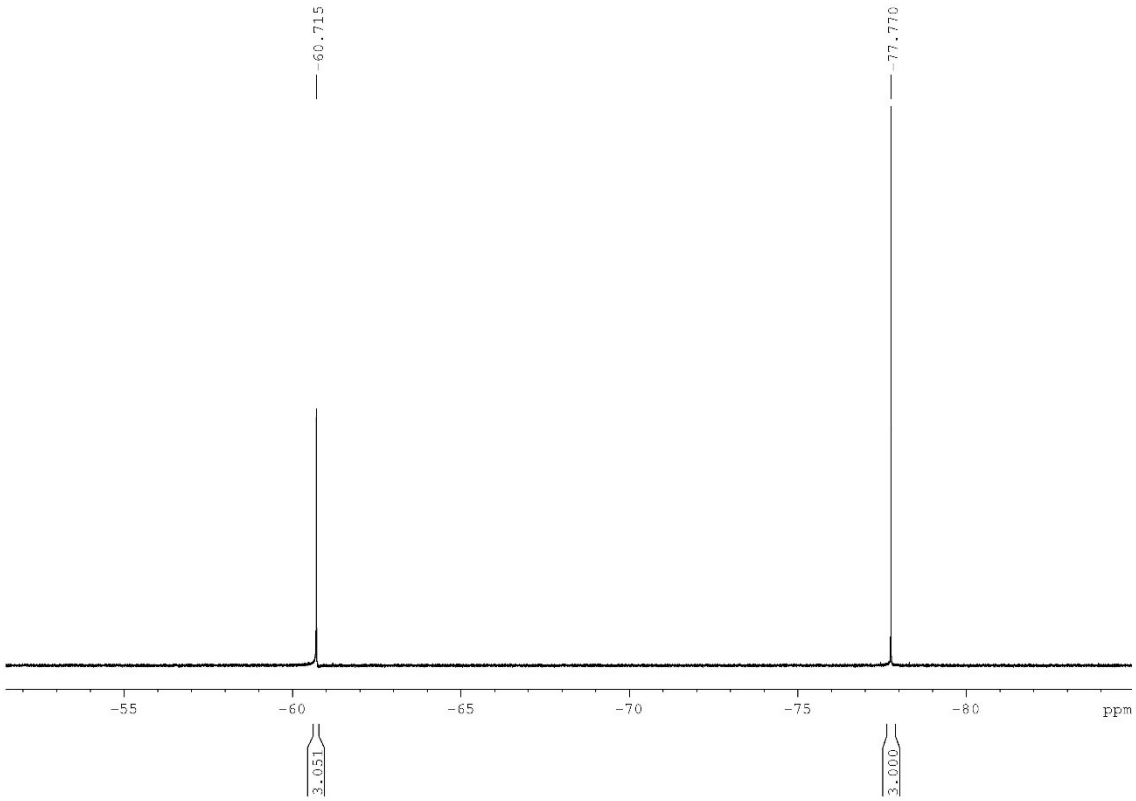

Figure S17. ^{19}F NMR spectrum of compound **Ru3** in DMSO-d_6

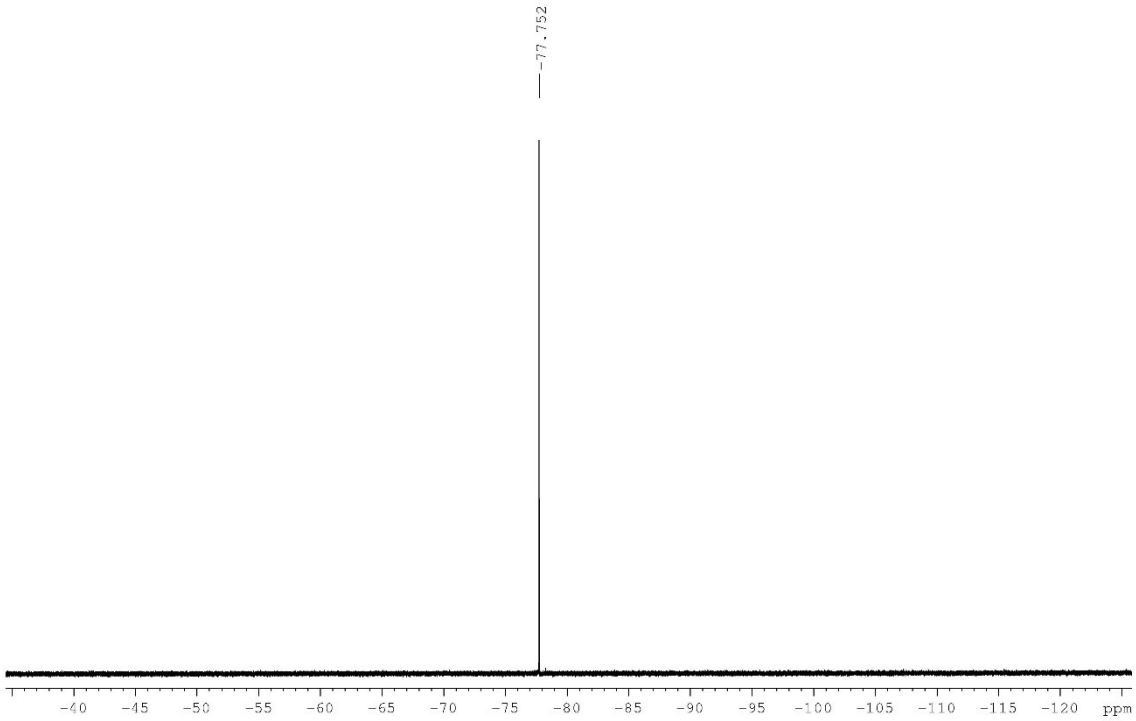

Figure S18. ^{19}F NMR spectrum of compound **Ru4** in DMSO-d_6

Table S1. HPLC method

Time (min)	0.1 % formic acid in H_2O	0.1 % formic acid in CH_3CN	Flow (mL/min)
0	80	20	0.4
25	0	100	

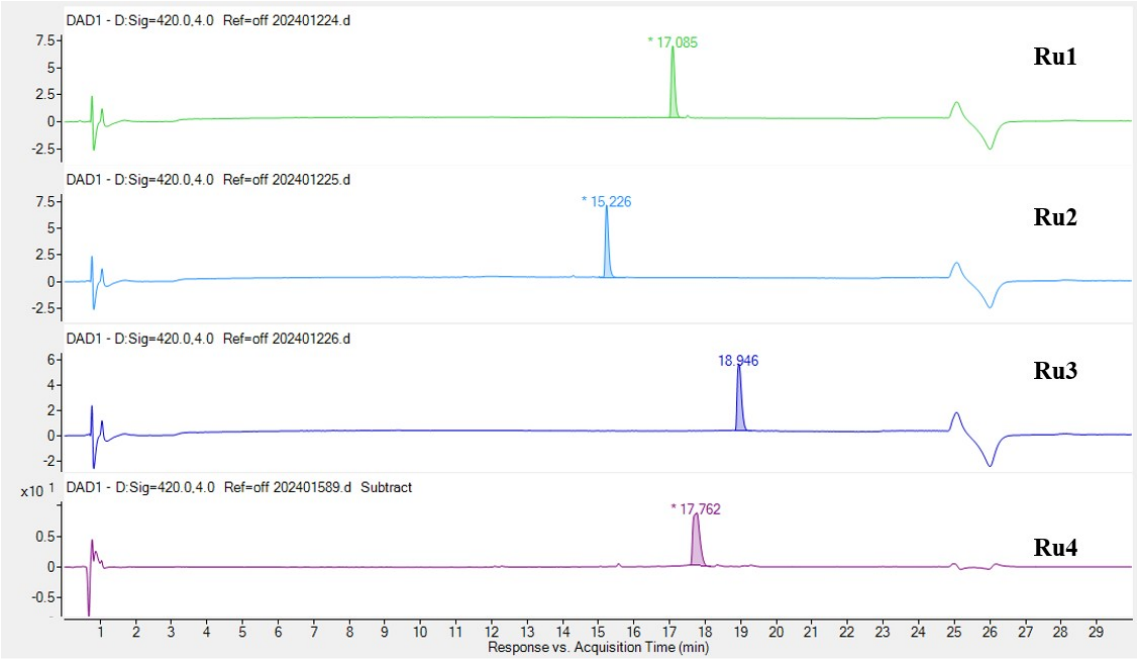

Figure S19. HPLC chromatograms with UV detection at 420 nm of complexes **Ru1-Ru4**

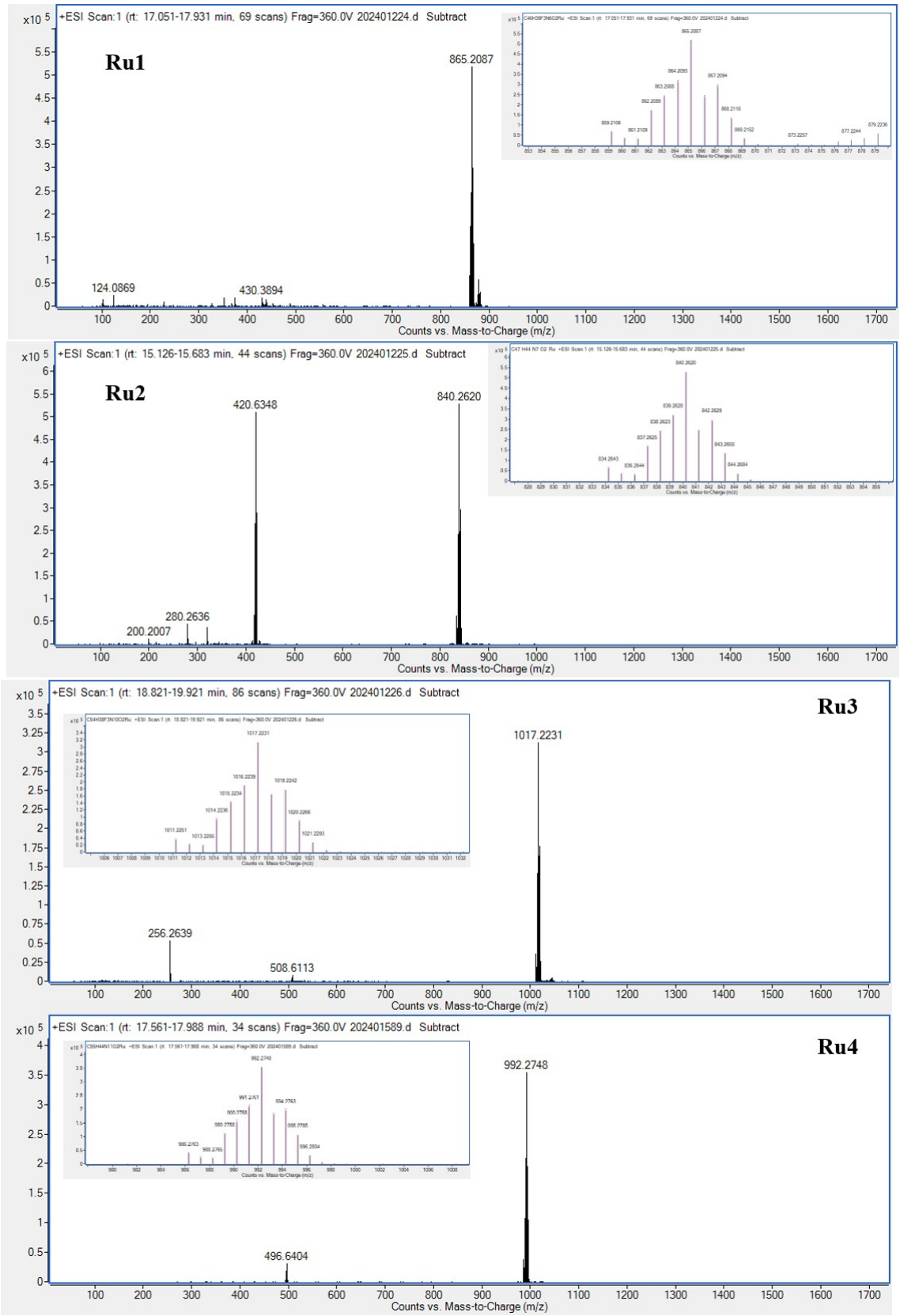

Figure S20. Mass spectra of the 15-18 min peak of chromatograms of **Figure S19** corresponding to the complexes.

Table S2. Crystal data and structure refinement of complex **Ru2**

Empirical formula	$C_{47}H_{44}N_7O_2Ru.CF_3O_3S.1(CH_2Cl_2).0.5(C_4H_{10}O).1.75[H_2O]$	
Formula weight	1142.54	
Temperature	100(2) K	
Wavelength	0.71073 Å	
Crystal system	Triclinic	
Space group	P-1	
Unit cell dimensions	a = 13.5090(6) Å	α = 84.3410(10)°
	b = 14.0322(7) Å	β = 73.105(2)°
	c = 15.9709(6) Å	γ = 62.2960(10)°
Volume	2562.3(2) $Å^3$	
Z	2	
Density (calculated)	1.481 Mg/m^3	
Absorption coefficient	0.521 mm^{-1}	
F(000)	1177	
Crystal size	0.290 x 0.230 x 0.120 mm^3	
Theta range for data collection	1.641 to 27.103°	
Index ranges	-17<=h<=17, -17<=k<=17, -20<=l<=20	
Reflections collected	184861	
Independent reflections	11300 [R(int) = 0.0273]	
Completeness to theta = 26.000°	100.0 %	
Refinement method	Full-matrix least-squares on F2	
Data / restraints / parameters	11300 / 32 / 691	
Goodness-of-fit on F2	1.058	
Final R indices [I>2sigma(I)]	R1 = 0.0610, wR2 = 0.1684	
R indices (all data)	R1 = 0.0629, wR2 = 0.1704	
Largest diff. peak and hole	1.844 and -2.047 $e.Å^{-3}$	

Table S3. Hydrogen bonds for **Ru2** [Å and °]

	D-H...A	d(D-H)	d(H...A)	d(D...A)<(DHA)
C(11)-H(11A)...O(98)#1	0.99	2.52	3.395(7)	147.3
C(34)-H(34)...O(98)#2	0.95	2.53	3.407(6)	153.4
C(41)-H(41)...O(96)	0.95	2.38	3.273(6)	157.3
C(81)-H(81A)...O(96)#4	0.99	2.57	3.549(10)	170.9

Symmetry transformations used to generate equivalent atoms:

#1 -x+1,-y+2,-z+1 #2 x+1,y-1,z #3 x,y-1,z #4 -x,-y+2,-z+1

Photophysical properties

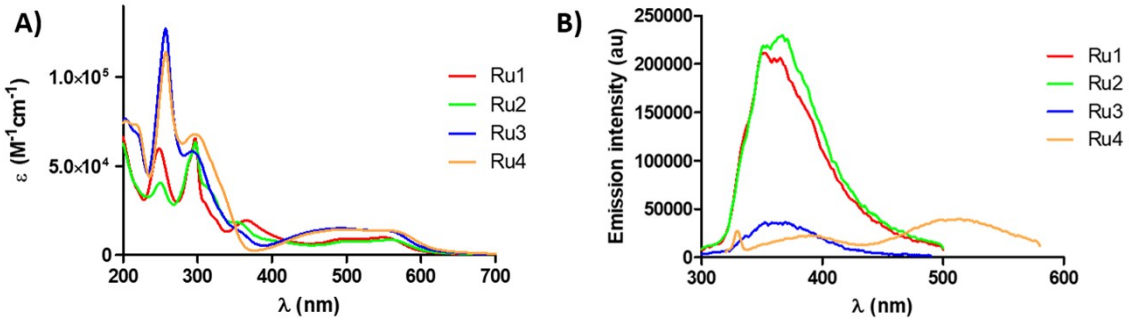

Figure S21. A) UV/vis spectra of compounds **Ru1-Ru4 (**10 μM) in acetonitrile. B) Emission spectra of **Ru1-Ru4 (**10 μM) in acetonitrile. **Ru1-Ru3**: λ_{ex}= 255 nm; **Ru4**: λ_{ex}= 300 nm.

Table S4. Absorption wavelengths (λ_{abs}) and molar extinction coefficient (ε) of absorption spectra of the complexes **Ru1-Ru4** in acetonitrile and water (1% DMSO)

Complex	**Solvent**	**λ (nm) (ε, M^{-1}cm^{-1})**
Ru1	H_2O (1% DMSO)	298 (68710), 373 (21290), 494 (11060), 549 (11960)
	CH_3CN	297 (65610), 370 (19150), 500 (9130), 550 (9940)
Ru2	H_2O (1% DMSO)	299 (73960), 351 (24340), 498 (10240), 560 (11020)

	CH_3CN	297 (63470), 351 (18520), 504 (7810), 558 (8630)
Ru3	H_2O (1% DMSO)	258 (117870), 295 (59550), 494 (16480), 548 (16590)
	CH_3CN	257 (127210), 293 (58210), 498 (15080), 551 (14000)
Ru4	H_2O (1% DMSO)	259 (10538), 296 (65380), 493 (15020), 562 (14760)
	CH_3CN	257 (114280), 302 (66860), 500 (14570), 554 (13810)

Stability studies

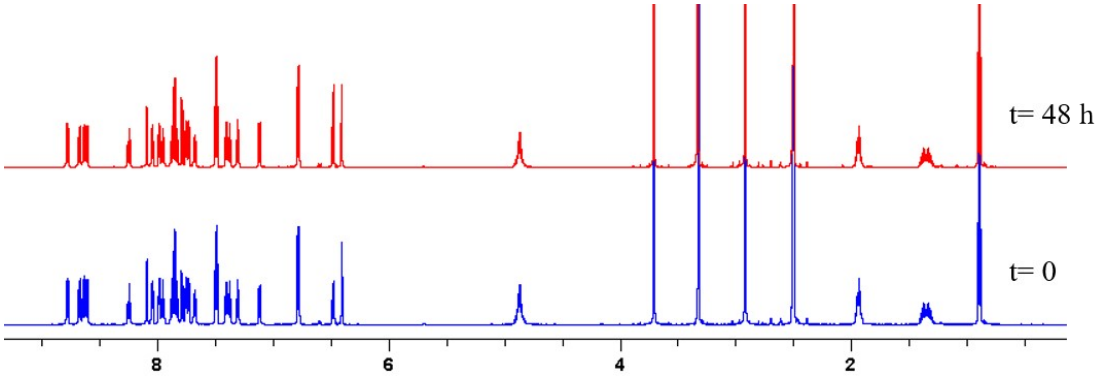

Figure S22. ^{1}H NMR spectra of compound **Ru2** in DMSO at t = 0 and after 48 h.

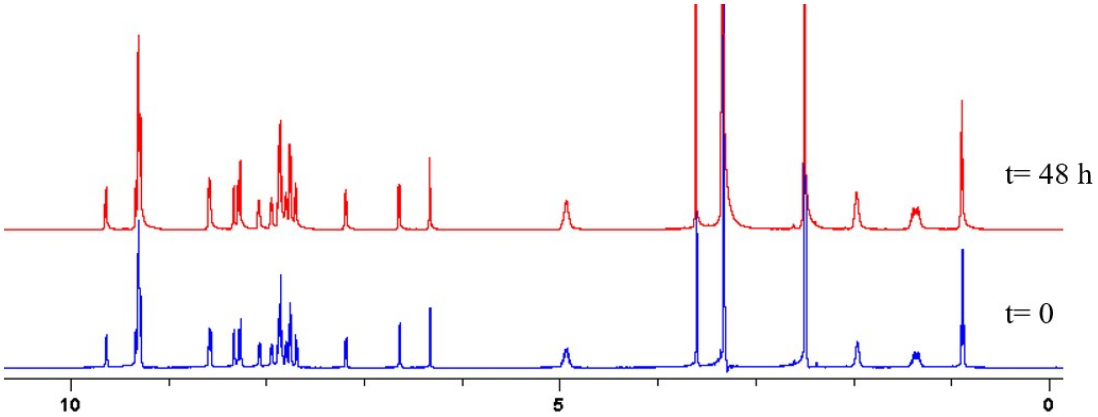

Figure S23. ^{1}H NMR spectra of compound **Ru3** in DMSO at t = 0 and after 48 h.

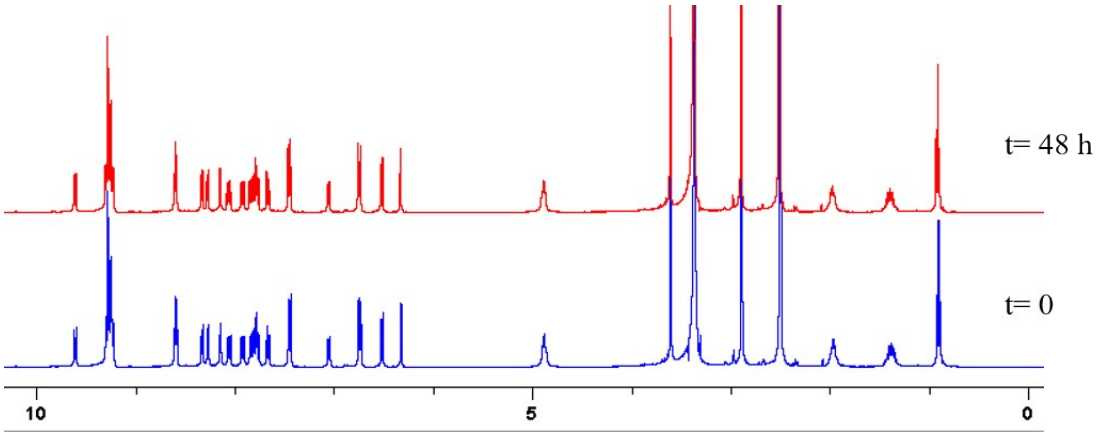

Figure S24. ^{1}H NMR spectra of compound **Ru4** in DMSO at t = 0 and after 48 h.

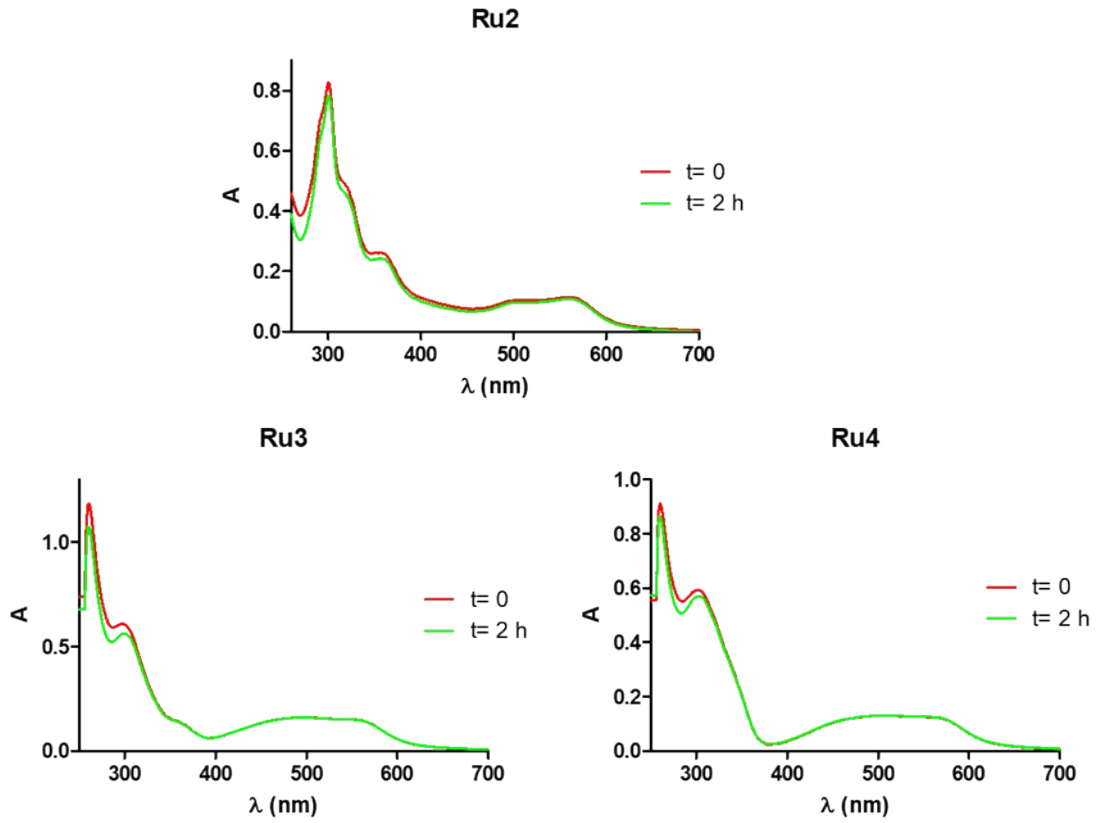

Figure S25. Time evolution of the absorption spectra of **Ru2** –**Ru4** (10 μM) in DMSO solution upon exposure to green light (1.8 mW/cm^2) during 2 h.

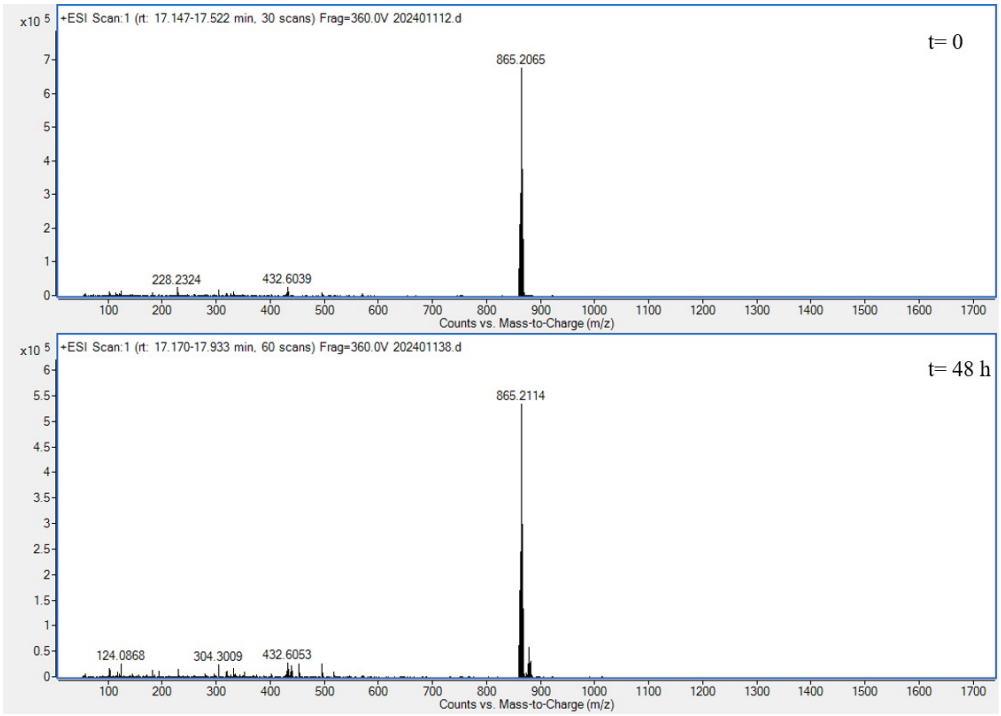

Figure S26. ESI-MS from HPLC of Figure 4C (**Ru1** (10 μM)) in DMEM (5% DMSO) with 10 % FBS at t = 0 and after 48 hours and incubated at 37 ºC.

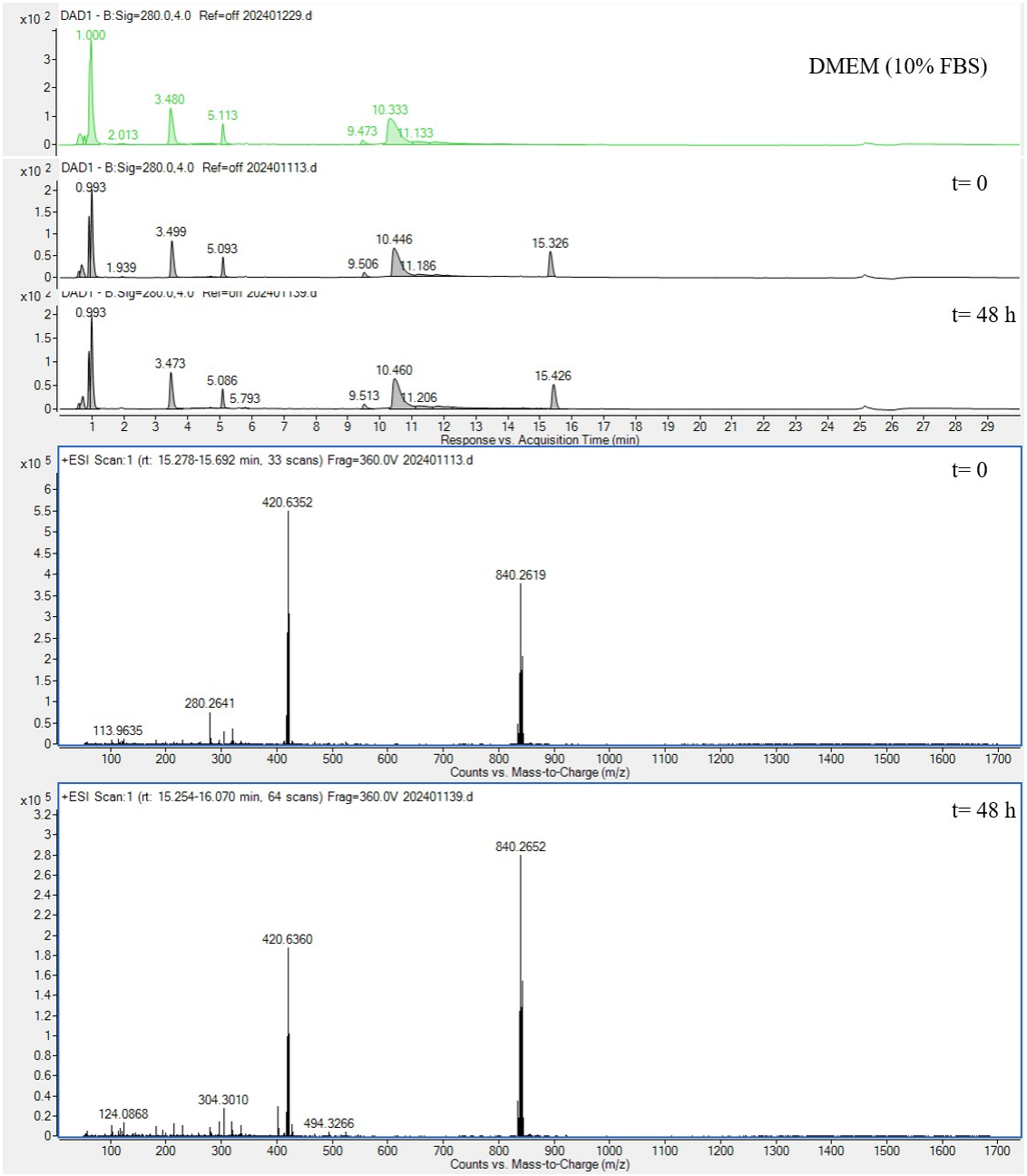

Figure S27. HPLC-MS of **Ru2** (10 μM) in DMEM (5% DMSO) with 10 % FBS at t = 0 and after 48 hours and incubated at 37 ºC.

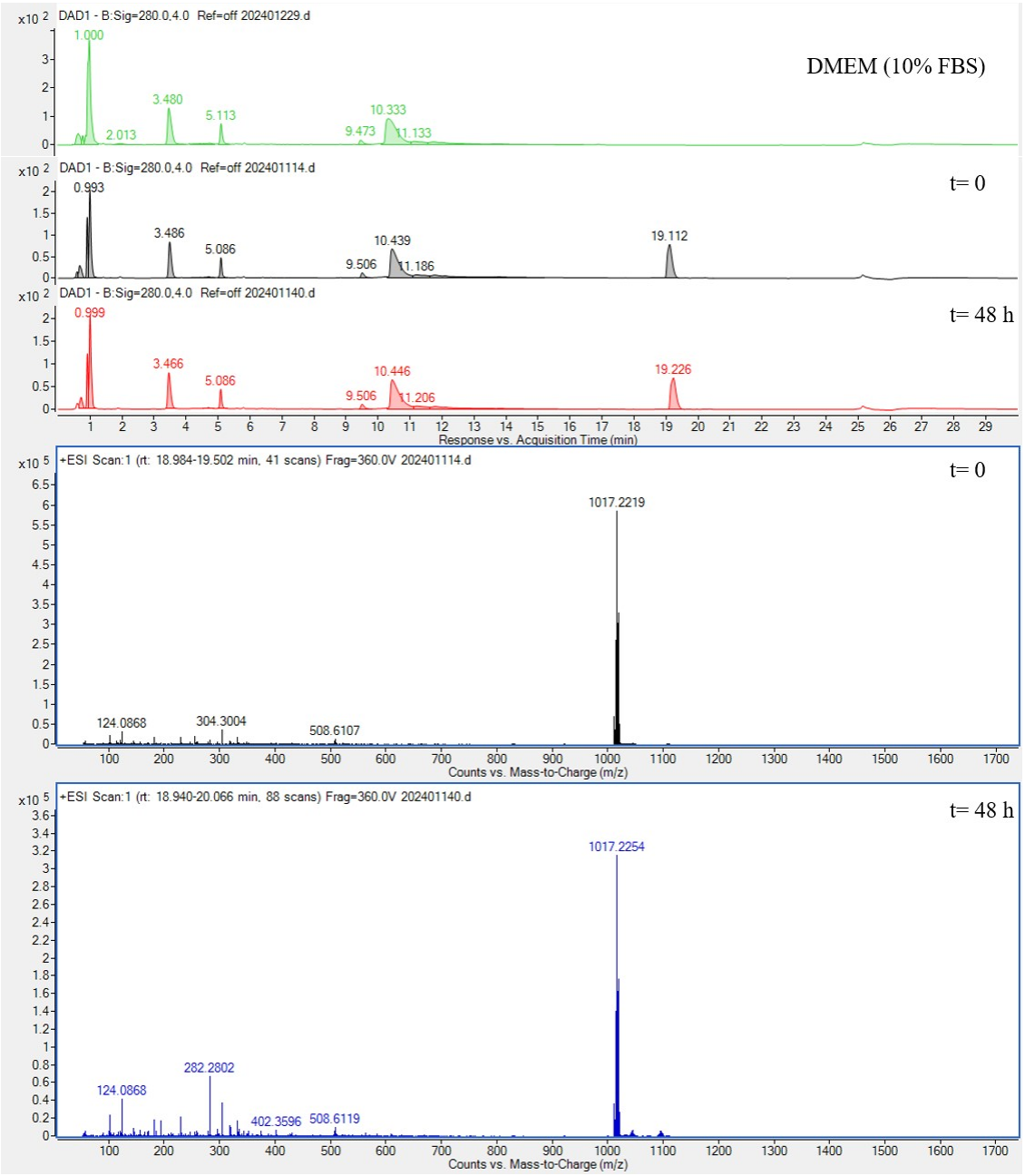

Figure S28. HPLC-MS of **Ru3** (10 μM) in DMEM (5% DMSO) with 10 % FBS at t = 0 and after 48 hours and incubated at 37 ºC

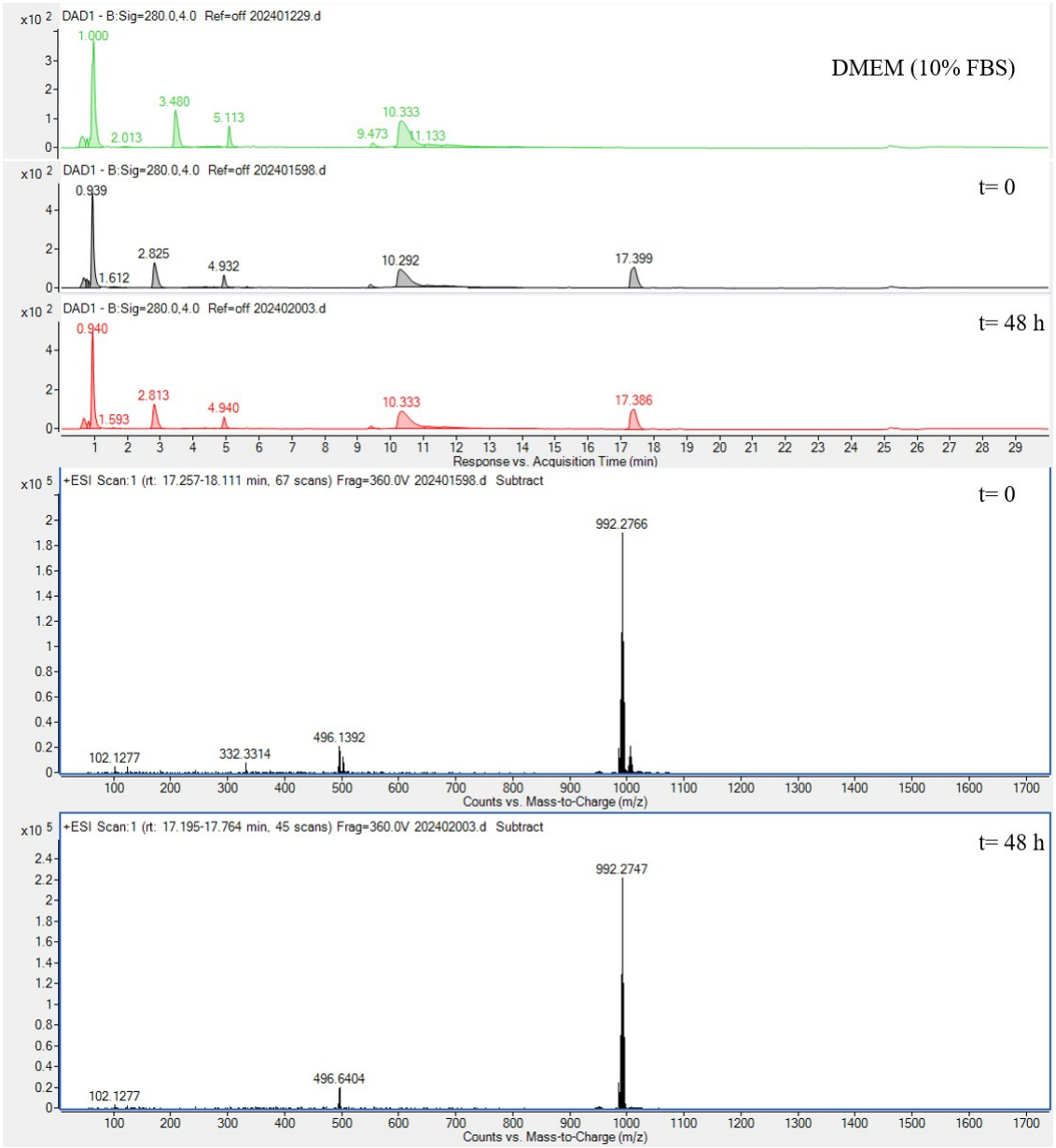

Figure S29. HPLC-MS of **Ru4** (10 μM) in DMEM (5% DMSO) with 10 % FBS at t = 0 and after 48 hours and incubated at 37 ºC.

Reaction with Human Serum Albumin (HSA).

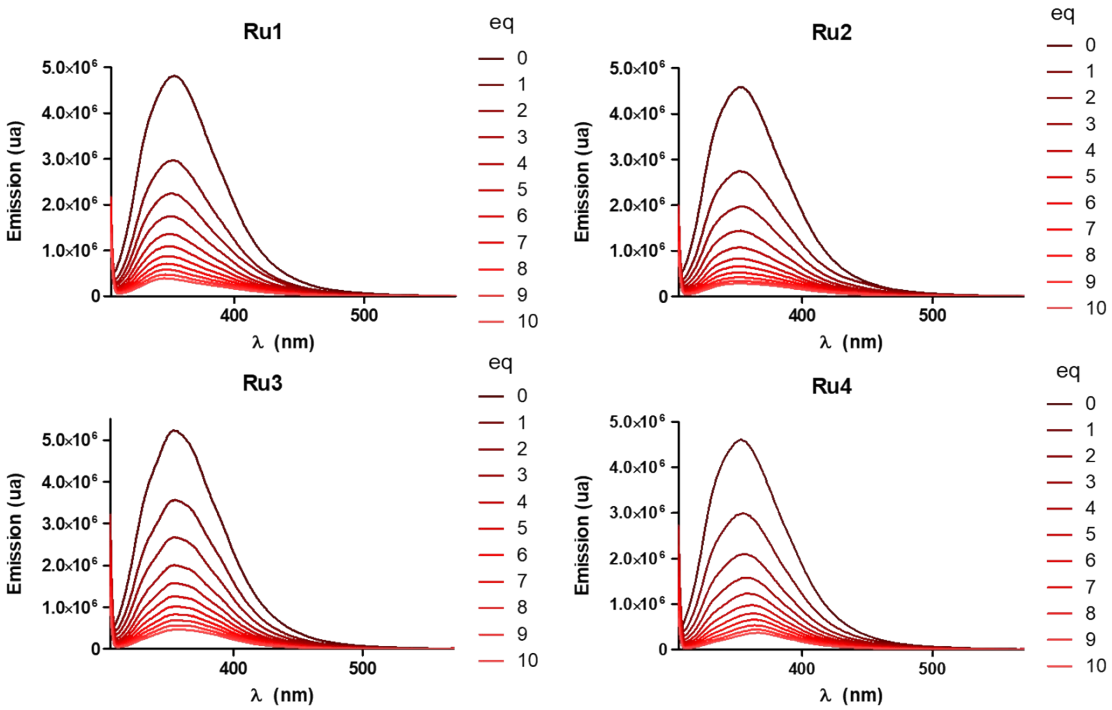

Figure S30. Emission spectra of HSA (2.5 μM) in the presence of increasing amounts of **Ru1-Ru4** complexes (0-25 μM)

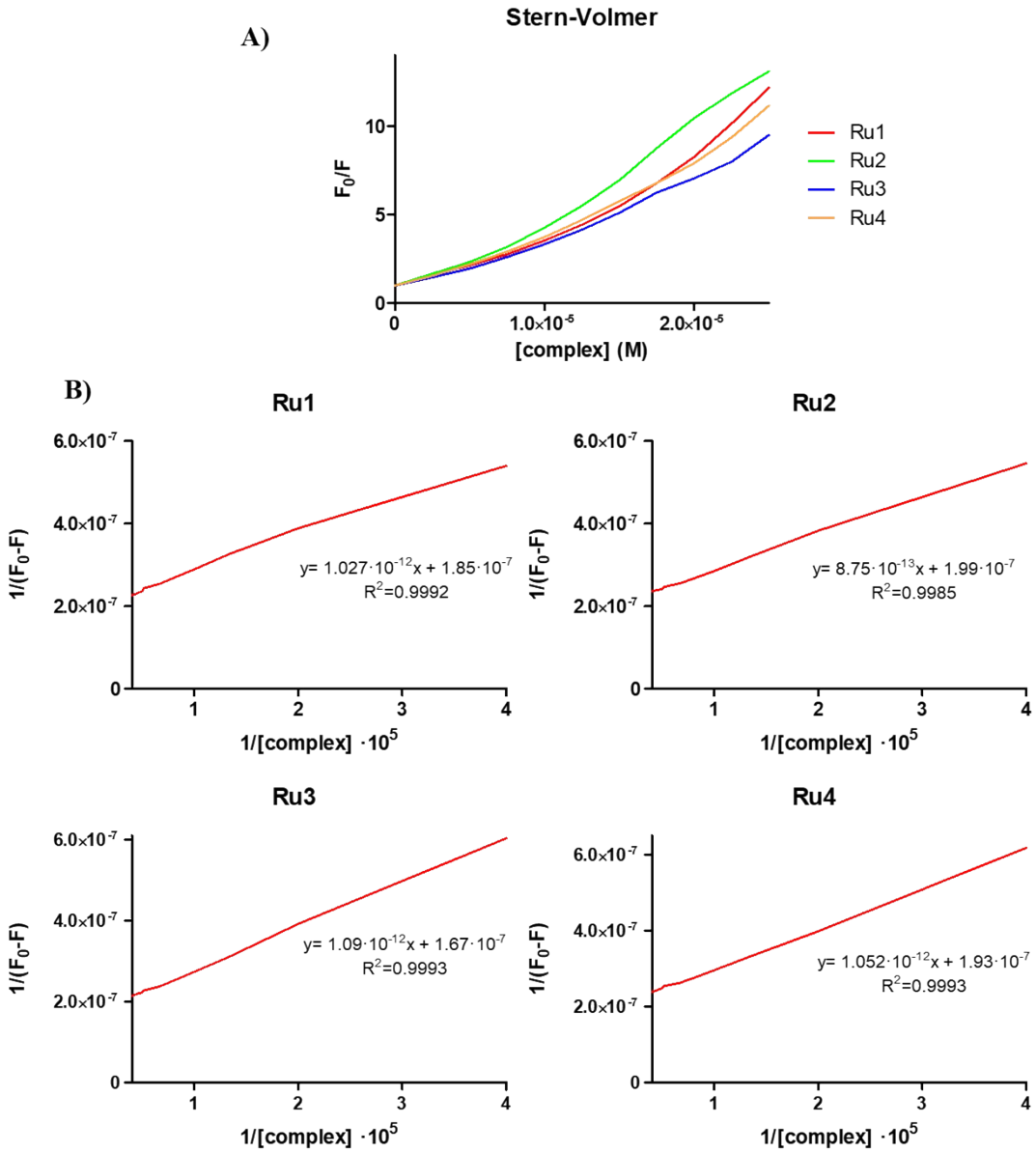

Figure S31. A) Stern-Volmer and **B**) Lineweaver-Burk curves of the quenching of HSA fluorescence in the presence of **Ru1-Ru4** complexes.

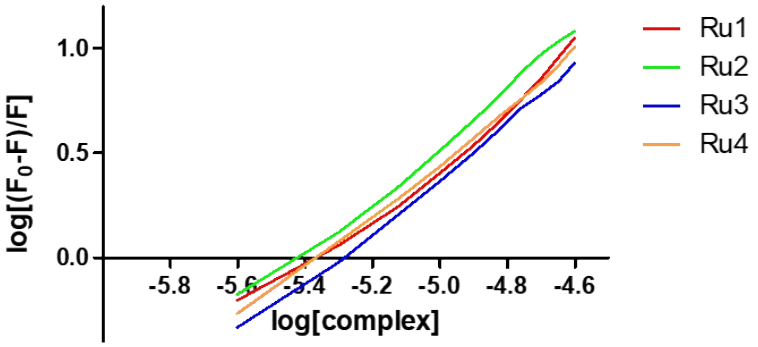

Figure S32. Scatchard curves for **Ru1-Ru4** complexes

6. Evaluation for $^1O_2$ and/or •OH generation in cell free media.

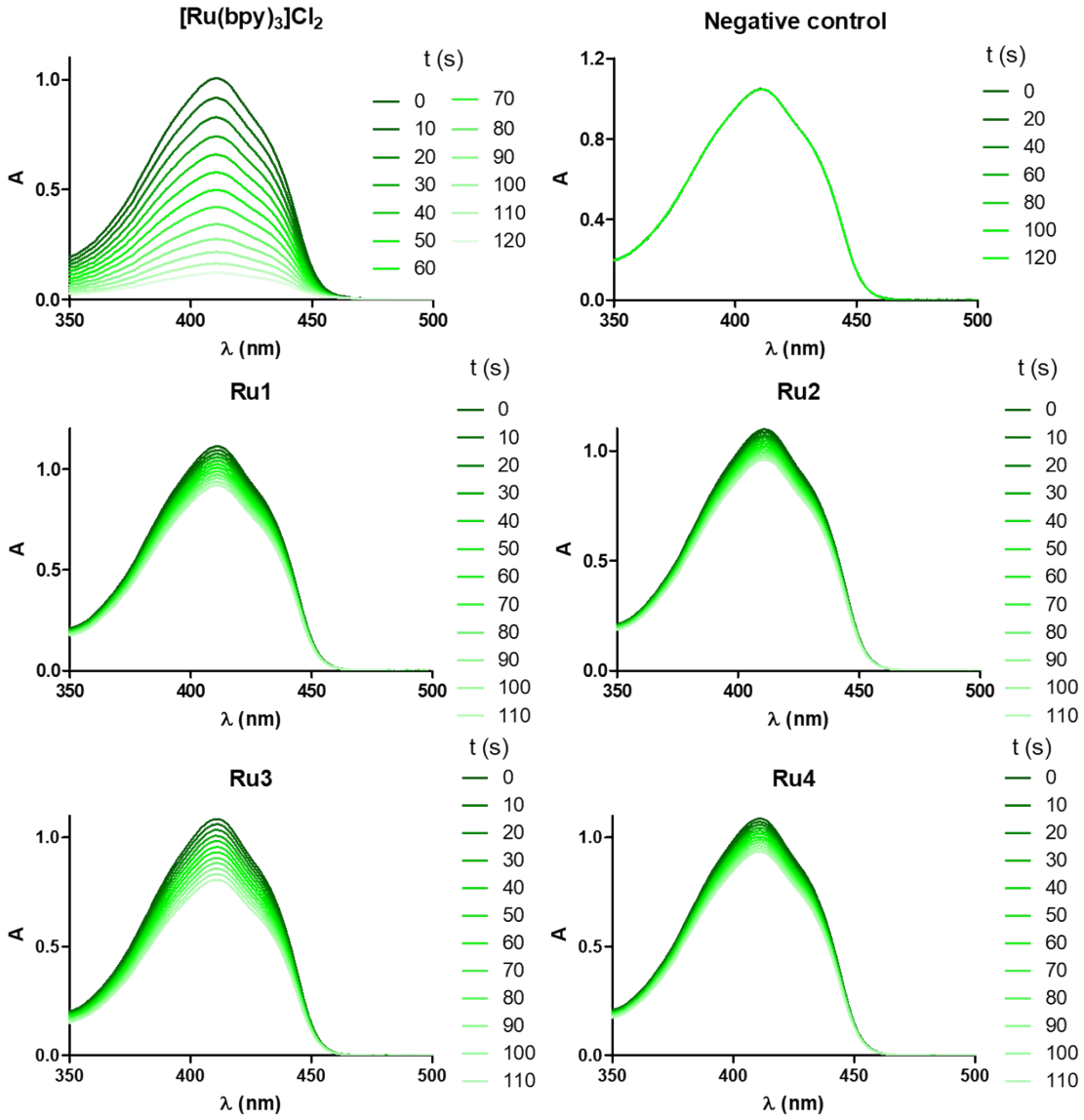

Figure S33. Absorbance decrease of DPBF (50 μM) in presence of complexes **Ru1-Ru4** (4-7 μM) and the reference **$[Ru(bpy)_3]Cl_2$** (50 μM) in aerated acetonitrile when irradiating with green light (520 nm, 0.5 mW/cm^2). Acetonitrile was used as a negative control.

Table S5. Singlet oxygen quantum yields

Complex	ϕ
Ru1	0.13
Ru2	0.078
Ru3	0.15
Ru4	0.093

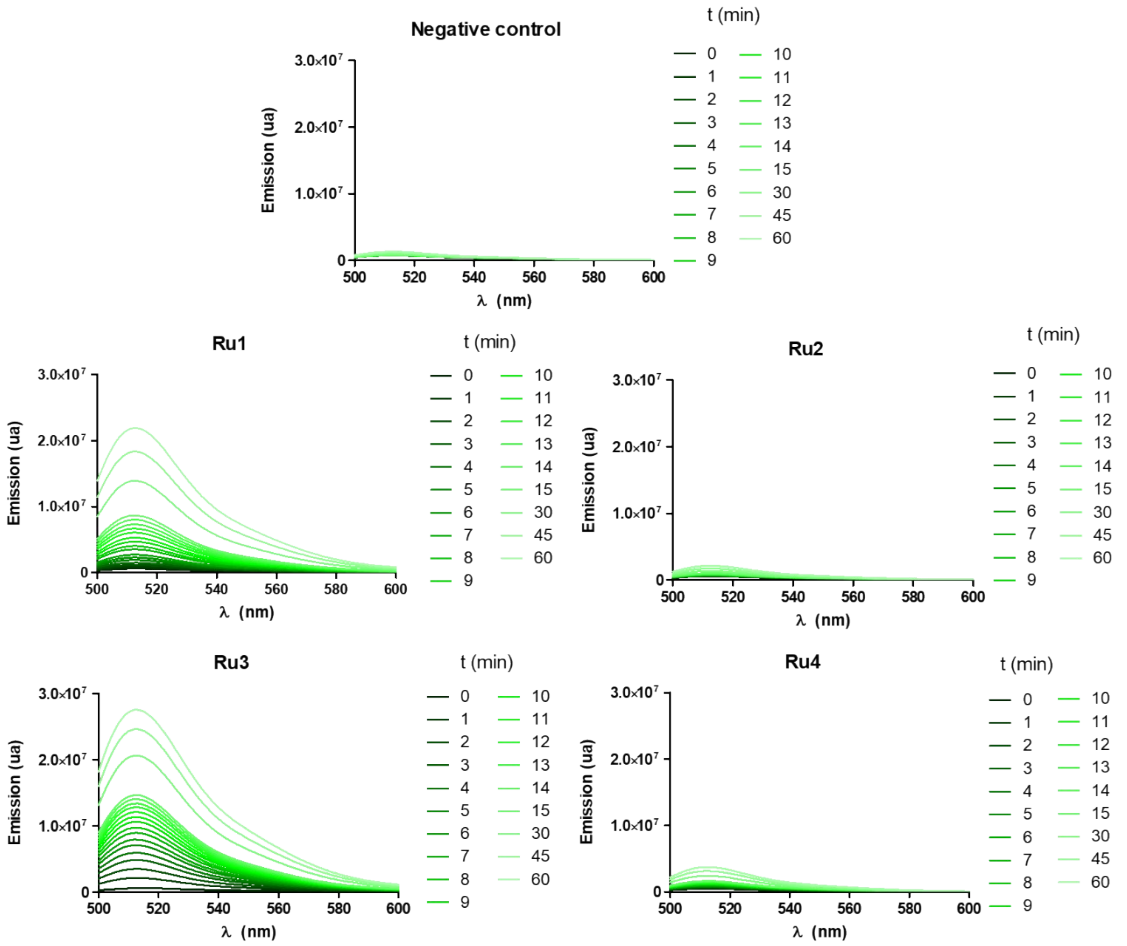

Figure S34. Increase of the fluorescence spectra emission of HPF upon photoirradiation of Ru(II) complexes Ru1-Ru4 at 520 nm (2 mW/cm^2) in PBS (5 % DMF). HPF fluorescence was excited at 490 nm. PBS (5 % DMF) was used as a negative control.

7. Biological assays

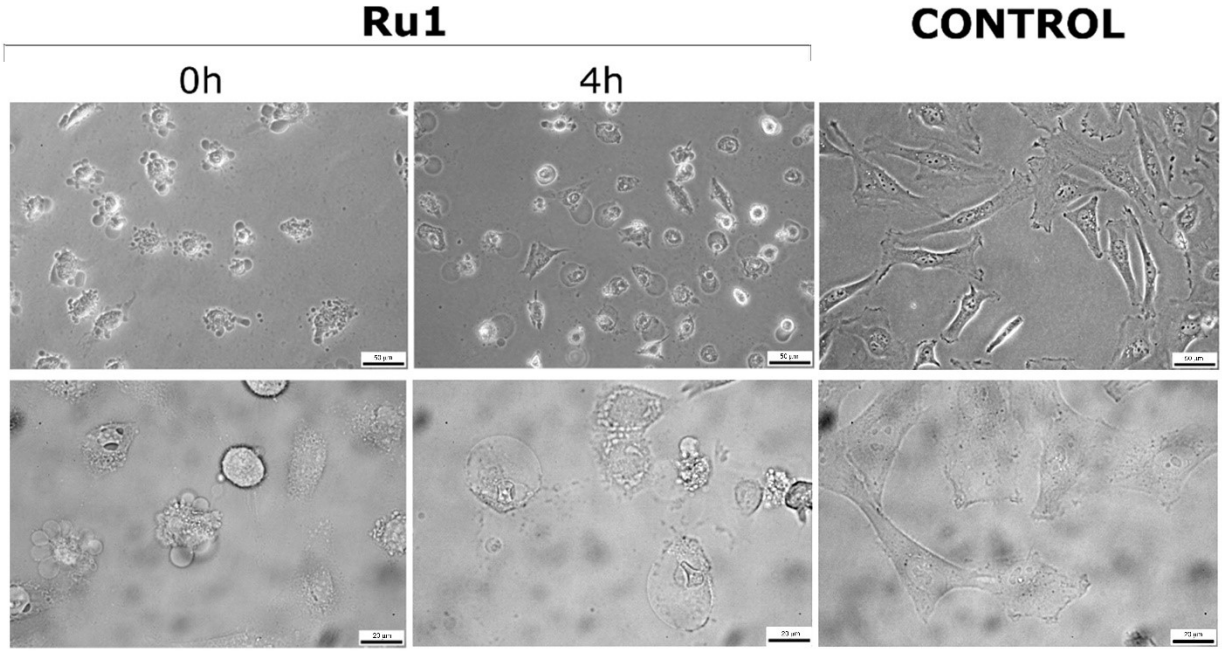

Figure S35. Microscopic images of HeLa cell morphology, vacuolization of cytoplasm, and cell swelling, as revealed by an inverted optical microscope. Cells were treated with **Ru1** (concentration corresponding to IC_{50}, Table 2) or untreated (control), irradiated and photographed immediately after irradiation (0h) or after 4 h recovery in cell free media Scale bars represent 50 μm (top panels) or 20 μm (bottom panels).

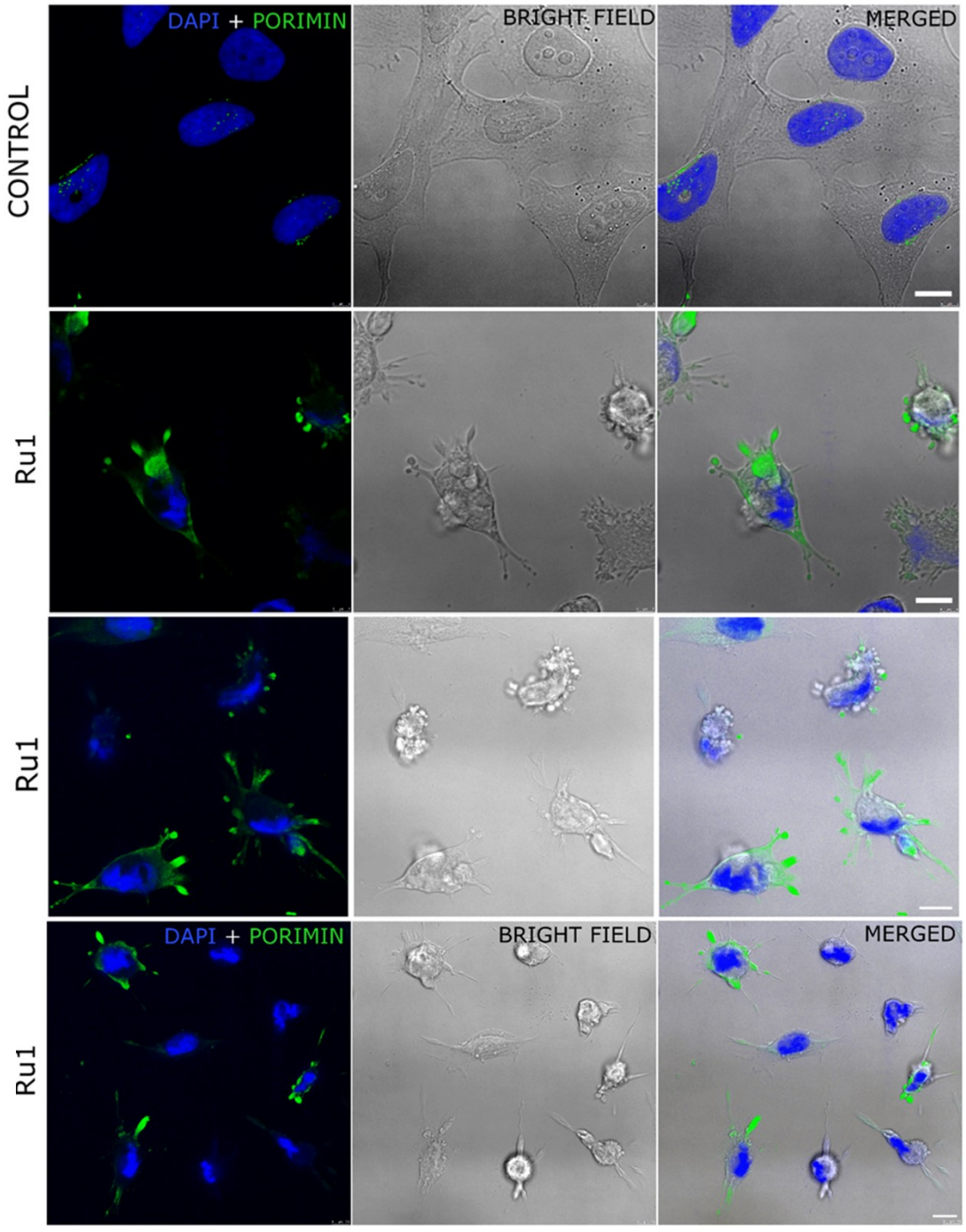

Figure S36. Immunofluorescence staining of Hela cells showing membrane localization of Porimin (green fluorescence signal); for better clarity, nuclei were stained with DAPI (blue signal). Top row: Control, untreated cells 4h after irradiation. Ru1: Cells treated with **Ru1** in a concentration corresponding IC_{50} (Table 2) 4 h after irradiation. Three representative images are shown. Scale bars represent 10 μm.

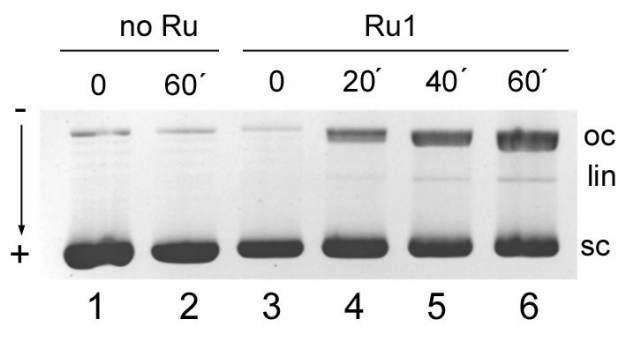

Figure S37. DNA photo-cleavage by **Ru1**. Plasmid pBR322 was mixed with the Ru complex **Ru1** (concentration ratio [Ru]/[DNA] = 1/10). Samples were irradiated with a green light for the indicated time. Control, untreated DNA irradiated for 0 and 60 min was also included in the experiment (lanes 1 and 2). In both panels, the top DNA bands correspond to the nicked plasmid (OC), and the bottom bands correspond to the negatively supercoiled plasmid (SC). Linear DNA (lin) also appears in the samples treated with **Ru1** as a result of the formation of single-strand breaks in the close vicinity.

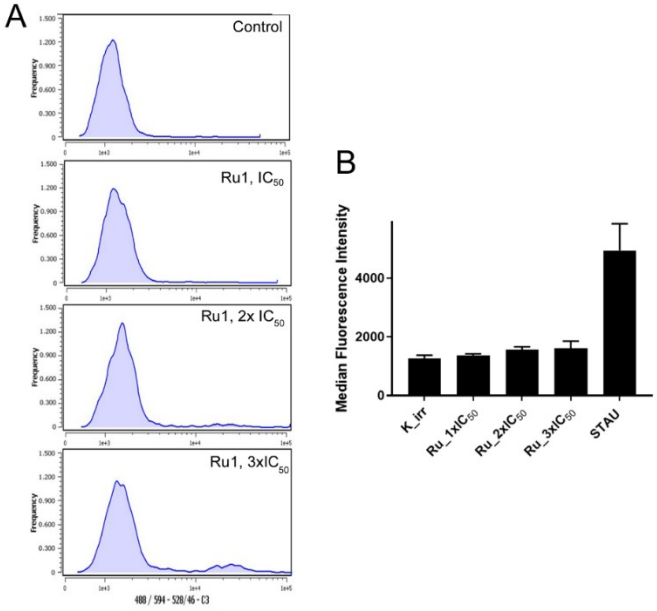

Figure S38. Activation of caspase 3/7 detected by CellEvent®Caspase3/7 Green Detection Reagent. HeLa cells were treated with **Ru1** (or incubated untreated) for 1 h in the dark and irradiated with green light. After 24 h of recovery in compound-free media, cell samples were stained with the CellEvent®Caspase 3/7 Green Detection Reagent, and fluorescence was analyzed by flow-cytometry; 30 000 cells were analyzed in each sample. A. Representative histograms. B. Quantitative evaluation. In the highest concentration (corresponding to 3x IC_{50}, a negligible amount of apoptotic cells are

detected; however, the apoptotic population is not significantly different from that in control, untreated irradiated cells. As a positive control, staurosporine (STAU, 1μM) was included in the experiment.

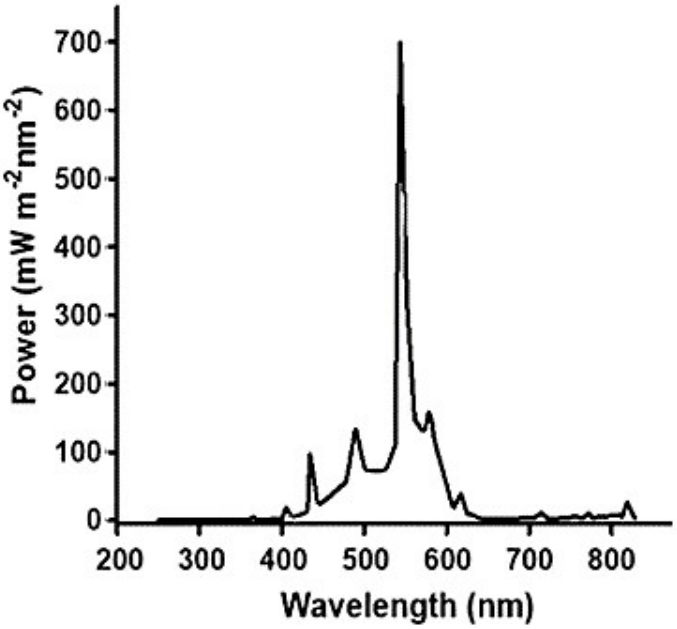

Figure S39. Spectral characteristic of green light used in the biological experiments.

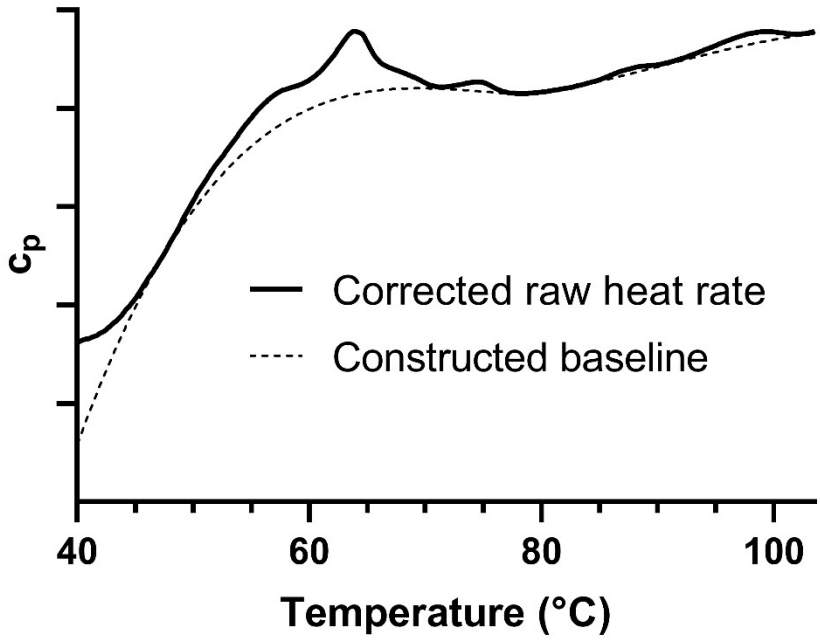

Figure S40. The graph illustrates the construction of a baseline used to subtract background heat capacity in the evaluation of experiments conducted with differential scanning calorimetry.

References

(1) Hernández-García, A.; Marková, L.; Santana, M. D.; Prachařová, J.; Bautista, D.; Kostrhunová, H.; Novohradský, V.; Brabec, V.; Ruiz, J.; Kašpárková, J. Cyclometalated Benzimidazole Osmium(II) Complexes with Antiproliferative Activity in Cancer Cells Disrupt Calcium Homeostasis. *Inorg. Chem.* **2023**, *62* (16), 6474–6487. https://doi.org/10.1021/acs.inorgchem.3c00501.

(2) Yellol, J.; Pérez, S. A.; Buceta, A.; Yellol, G.; Donaire, A.; Szumlas, P.; Bednarski, P. J.; Makhloufi, G.; Janiak, C.; Espinosa, A.; Ruiz, J. Novel C,N-Cyclometalated Benzimidazole Ruthenium(II) and Iridium(III) Complexes as Antitumor and Antiangiogenic Agents: A Structure–Activity Relationship Study. *J. Med. Chem.* **2015**, *58* (18), 7310–7327. https://doi.org/10.1021/acs.jmedchem.5b01194.

(3) Ballester, F. J.; Ortega, E.; Bautista, D.; Santana, M. D.; Ruiz, J. Ru(II) Photosensitizers Competent for Hypoxic Cancers via Green Light Activation. *Chem. Commun.* **2020**, *56* (71), 10301–10304. https://doi.org/10.1039/D0CC02417A.